Neural Network Engine

A Comprehensive Deep Learning Framework with Automatic Differentiation

and Research Software for Neural Network Education & Experimentation

Matt

Varna, Bulgaria

July 22, 2025

Abstract

The Neural Network Engine is a comprehensive machine learning framework built from first principles, implementing core deep learning concepts through practical, educational code. The engine features nine activation functions including ReLU, Sigmoid, Tanh, and advanced variants like Swish and GELU, paired with robust optimization algorithms including SGD with momentum and Adam optimizer.

The framework supports complete neural network workflows from data preprocessing through model training and evaluation. Three applications demonstrate its capabilities: a high-accuracy digit recognition system with interactive visualization, a universal character recognizer handling alphanumeric classification, and an innovative quadratic equation predictor exploring neural networks in mathematical problem-solving.

Key contributions include numerically stable implementations, automatic differentiation for gradient computation, modular architecture enabling rapid experimentation, and comprehensive performance monitoring tools. The engine successfully bridges theoretical understanding with practical implementation, making complex deep learning concepts accessible while providing robust tools for real-world pattern recognition and classification tasks.

Contents

Chapter 1

Theoretical Foundations

Neural networks form the cornerstone of modern artificial intelligence, representing sophisticated mathematical models capable of learning complex patterns from data. This chapter establishes the theoretical foundations underlying the Neural Network Engine, exploring both the fundamental principles of neural computation and the mathematical frameworks enabling efficient optimization. The theoretical understanding presented here provides the essential groundwork for comprehending the advanced implementation details and practical applications documented in subsequent chapters.

1.1 Neural Networks Fundamentals

1.1.1 Historical Context and Biological Inspiration

Neural networks draw inspiration from biological neural systems, where interconnected neurons process and transmit information through electrochemical signals. The mathematical formalization of these concepts began with McCulloch and Pitts in 1943, who demonstrated that networks of simple artificial neurons could perform logical operations. This foundational work established the theoretical basis for modern neural computation, proving that appropriately connected networks of binary threshold units could compute any logical function.

In artificial neural networks, this biological concept translates to computational models composed of interconnected processing units called **neurons** or **nodes**, each performing simple mathematical operations while collectively enabling complex pattern recognition and function approximation. The fundamental principle underlying neural networks is the concept of **distributed representation**, where information is encoded across multiple neurons rather than within individual units. This approach enables robust learning, generalization to unseen data, and fault tolerance—characteristics that make neural networks particularly effective for real-world applications.

The theoretical foundation for neural networks' computational power rests on several key mathematical principles. First, the **superposition principle** allows complex functions to be represented as weighted combinations of simpler functions. Second, the concept of **hierarchical feature learning** enables networks to automatically discover increasingly abstract representations through multiple layers of transformation. Third, the **non-linear composition** of simple operations creates systems capable of approximating arbitrarily complex mappings between input and output spaces.

1.1.2 Network Architecture and Mathematical Structure

A neural network consists of multiple **layers** of interconnected neurons, typically organized in a feedforward architecture. The mathematical structure of these networks can be

precisely defined through a series of transformations operating on vector spaces.

Input Layer: Receives raw data features, with each neuron corresponding to a specific input dimension. For a dataset with n features, the input layer contains n neurons representing the feature vector $\mathbf{x} = [x_1, x_2, \ldots, x_n]^T \in \mathbb{R}^n$.

Hidden Layers: Intermediate layers that transform input data through learned representations. Each hidden layer l contains h_l neurons, where the number of layers L and neurons per layer constitute the network's **architecture**. The architectural space can be formally defined as:

$$\mathcal{A} = \{(h_1, h_2, \ldots, h_L) : h_i \in \mathbb{N}^+, L \in \mathbb{N}^+\} \tag{1.1}$$

Output Layer: Produces the final predictions, with the number of neurons determined by the specific task. For regression tasks with m outputs, the output layer contains m neurons producing $\hat{\mathbf{y}} \in \mathbb{R}^m$. For classification tasks with C classes, the output typically consists of C neurons representing class probabilities.

Weights and Biases: Each connection between neurons is associated with a **weight** w_{ij} representing the strength of the connection from neuron i to neuron j. The weight matrix for layer l is denoted $\mathbf{W}^{(l)} \in \mathbb{R}^{h_l \times h_{l-1}}$, where $h_0 = n$ (input dimension). Additionally, each neuron has a **bias** term b_j that shifts the activation function, collected in bias vector $\mathbf{b}^{(l)} \in \mathbb{R}^{h_l}$.

The total parameter space of a neural network is given by:

$$\Theta = \bigcup_{l=1}^{L} \{\mathbf{W}^{(l)}, \mathbf{b}^{(l)}\} \tag{1.2}$$

with dimensionality:

$$|\Theta| = \sum_{l=1}^{L} (h_l \times h_{l-1} + h_l) = \sum_{l=1}^{L} h_l(h_{l-1} + 1) \tag{1.3}$$

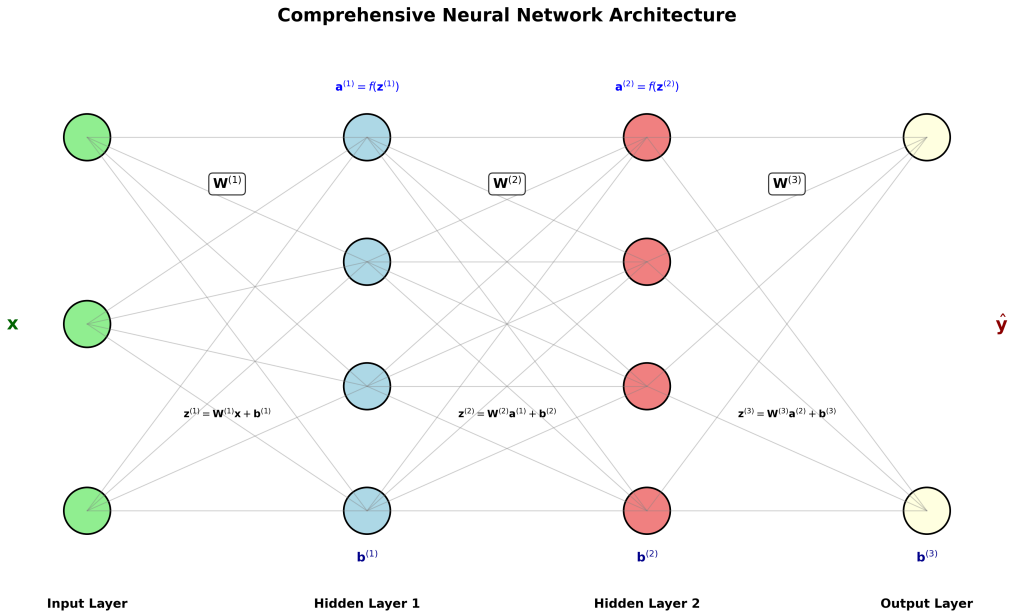

Figure 1.1: Fundamental neural network architecture showing input layer, hidden layers, and output layer with interconnected neurons. Weights and biases control information flow between layers.

1.1.3 Forward Propagation Mechanics and Mathematical Framework

Forward propagation represents the process by which input data flows through the network to produce predictions. This process can be mathematically described as a composition of affine transformations followed by non-linear activations.

For a layer l with input $\mathbf{a}^{(l-1)}$, the computation proceeds in two distinct stages:

Linear Transformation: The weighted sum of inputs plus bias terms:

$$\mathbf{z}^{(l)} = \mathbf{W}^{(l)}\mathbf{a}^{(l-1)} + \mathbf{b}^{(l)} \tag{1.4}$$

where $\mathbf{W}^{(l)} \in \mathbb{R}^{h_l \times h_{l-1}}$ represents the weight matrix for layer l, and $\mathbf{b}^{(l)} \in \mathbb{R}^{h_l}$ denotes the bias vector.

Nonlinear Activation: Application of an activation function $f^{(l)} : \mathbb{R} \to \mathbb{R}$ to introduce nonlinearity:

$$\mathbf{a}^{(l)} = f^{(l)}(\mathbf{z}^{(l)}) \tag{1.5}$$

where the activation function is applied element-wise to the vector $\mathbf{z}^{(l)}$.

The complete forward pass can be expressed as a composition of functions:

$$\hat{\mathbf{y}} = f^{(L)}(\mathbf{W}^{(L)}f^{(L-1)}(\mathbf{W}^{(L-1)} \cdots f^{(1)}(\mathbf{W}^{(1)}\mathbf{x} + \mathbf{b}^{(1)}) \cdots + \mathbf{b}^{(L-1)}) + \mathbf{b}^{(L)}) \tag{1.6}$$

The activation function enables neural networks to approximate nonlinear relationships, as composition of linear transformations alone can only represent linear functions regardless of network depth. The mathematical necessity of nonlinearity can be proven: without activation functions, any deep network reduces to:

$$\mathbf{y} = \left(\prod_{l=1}^{L} \mathbf{W}^{(l)}\right)\mathbf{x} + \mathbf{b}_{combined} \tag{1.7}$$

which is equivalent to a single-layer linear model.

1.1.4 Universal Approximation Theory

Neural networks function as **universal function approximators**, capable of approximating any continuous function to arbitrary precision given sufficient neurons and appropriate activation functions. This theoretical foundation, established by multiple formulations of the Universal Approximation Theorem, provides the mathematical justification for neural networks' effectiveness across diverse domains.

Cybenko's Theorem (1989): Let σ be a continuous, bounded, and non-constant activation function. Then finite linear combinations of the form:

$$G(x) = \sum_{j=1}^{N} \alpha_j \sigma(\mathbf{w}_j^T\mathbf{x} + b_j) \tag{1.8}$$

are dense in $C(I_n)$, the space of continuous functions on the unit hypercube $I_n = [0,1]^n$, with respect to the uniform norm.

Hornik's Generalization (1991): The universal approximation property holds for any bounded, non-constant activation function that is not a polynomial. This significantly broadens the class of admissible activation functions.

Modern Formulations: Recent work has extended these results to provide explicit bounds on approximation errors and required network width. For a function $f : [0,1]^n \to \mathbb{R}$ with bounded variation, there exists a neural network with one hidden layer containing at most $\mathcal{O}(\epsilon^{-n})$ neurons that approximates f within error ϵ.

The practical implications of these theorems are profound: - **Existence Guarantee**: For any continuous function on a compact domain, there exists a neural network that can approximate it arbitrarily well. - **Architecture Independence**: The approximation property depends primarily on width rather than depth for universal approximation. - **Activation Function Requirements**: The activation function must be non-polynomial and non-constant for universal approximation to hold.

However, these theorems do not address: - **Constructibility**: How to find the optimal weights and biases - **Efficiency**: The number of parameters required may be exponential in the input dimension - **Learnability**: Whether gradient-based methods can find good approximations

1.1.5 Loss Functions and Learning Objectives

The learning process involves optimizing a **loss function** $L(\mathbf{y}, \hat{\mathbf{y}})$ that measures the discrepancy between predicted outputs $\hat{\mathbf{y}}$ and true targets $\mathbf{y}$. The choice of loss function fundamentally shapes the learning dynamics and determines what aspects of the data the model emphasizes during training.

Mean Squared Error (MSE) for regression tasks:

$$L_{MSE} = \frac{1}{n}\sum_{i=1}^{n} \|\mathbf{y}_i - \hat{\mathbf{y}}_i\|^2 \tag{1.9}$$

The MSE loss assumes Gaussian noise in the data and corresponds to maximum likelihood estimation under this assumption. Its quadratic nature provides strong gradients far from the optimum but can be sensitive to outliers.

Cross-Entropy Loss for classification tasks:

$$L_{CE} = -\frac{1}{n}\sum_{i=1}^{n}\sum_{c=1}^{C} y_{i,c}\log(\hat{y}_{i,c}) \tag{1.10}$$

where C represents the number of classes, $y_{i,c}$ is the true label (one-hot encoded), and $\hat{y}_{i,c}$ is the predicted probability for class c.

Cross-entropy loss emerges naturally from the maximum likelihood principle when assuming categorical distributions. Its logarithmic nature provides strong gradients when predictions are incorrect and approaches zero when predictions are confident and correct.

Regularized Loss Functions: To prevent overfitting, regularization terms are often added to the base loss:

$$L_{total} = L_{data}(\mathbf{y}, \hat{\mathbf{y}}) + \lambda R(\Theta) \tag{1.11}$$

where $R(\Theta)$ is a regularization term and λ controls the regularization strength. Common regularization forms include: - **L1 Regularization**: $R(\Theta) = \sum_i |\theta_i|$ promotes sparsity - **L2 Regularization**: $R(\Theta) = \sum_i \theta_i^2$ penalizes large weights - **Elastic Net**: $R(\Theta) = \alpha\sum_i |\theta_i| + (1-\alpha)\sum_i \theta_i^2$ combines L1 and L2

1.1.6 Activation Functions and Their Mathematical Properties

Activation functions serve as the nonlinear elements that enable neural networks to learn complex patterns. Each activation function has distinct mathematical properties that affect network behavior, training dynamics, and representational capacity.

Sigmoid Function:

$$\sigma(z) = \frac{1}{1+e^{-z}}, \quad \sigma'(z) = \sigma(z)(1-\sigma(z)) \tag{1.12}$$

The sigmoid function maps inputs to $(0, 1)$ and has a smooth, S-shaped curve. However, its derivative is bounded by $[0, 0.25]$, leading to vanishing gradient problems in deep networks.

Hyperbolic Tangent:

$$\tanh(z) = \frac{e^z - e^{-z}}{e^z + e^{-z}}, \quad \tanh'(z) = 1 - \tanh^2(z) \tag{1.13}$$

Tanh maps inputs to $(-1, 1)$ and is zero-centered, which can improve convergence properties. Like sigmoid, it suffers from vanishing gradients due to its bounded derivative $[0, 1]$.

Rectified Linear Unit (ReLU):

$$\text{ReLU}(z) = \max(0, z), \quad \text{ReLU}'(z) = \begin{cases} 1 & \text{if } z > 0 \\ 0 & \text{if } z \leq 0 \end{cases} \tag{1.14}$$

ReLU addresses the vanishing gradient problem by providing a constant gradient of 1 for positive inputs. However, it can suffer from "dying ReLU" problem, where neurons become permanently inactive.

Advanced activation functions implemented in Neural Engine are detailed in Section 2.2, where we explore the mathematical properties and implementation considerations of various activation functions including ELU, Swish, and GELU variants.

1.1.7 Applications in Modern AI and Computational Complexity

Neural networks have revolutionized numerous domains through their ability to learn complex patterns from data. The theoretical foundations established above enable practical applications across diverse fields:

Computer Vision: Convolutional neural networks leverage translation equivariance and local connectivity to achieve superhuman performance in image recognition, object detection, and medical image analysis. The theoretical basis lies in the approximation of locally-varying functions through spatially-structured weight sharing.

Natural Language Processing: Transformer architectures have transformed language understanding through self-attention mechanisms that enable parallel computation of sequential dependencies. The mathematical foundation involves multi-head attention as learned similarity metrics in high-dimensional spaces.

Scientific Computing: Neural networks increasingly solve complex scientific problems, from protein folding prediction to climate modeling and quantum chemistry. Physics-informed neural networks (PINNs) incorporate differential equations directly into the loss function, enabling principled solutions to partial differential equations.

Control Systems: Deep reinforcement learning enables autonomous systems in robotics, game playing, and resource optimization through the marriage of neural function approximation with dynamic programming principles.

The computational complexity of neural network training scales as $\mathcal{O}(|\Theta| \cdot n \cdot T)$ where $|\Theta|$ is the number of parameters, n is the number of training examples, and T is the number of training iterations. Modern hardware accelerators (GPUs, TPUs) exploit the inherent parallelism in matrix operations to achieve practical training times for networks with millions or billions of parameters.

1.2 Automatic Differentiation Theory

1.2.1 Mathematical Foundations and Historical Development

Automatic differentiation forms the computational backbone of neural network training, enabling efficient calculation of gradients necessary for optimization algorithms. Unlike numerical differentiation, which suffers from approximation errors and requires $\mathcal{O}(n)$ function evaluations for n variables, automatic differentiation provides exact gradients with computational complexity proportional to the original function evaluation.

The fundamental principle relies on the mathematical fact that any computer program can be decomposed into a sequence of elementary mathematical operations (addition, multiplication, exponential, logarithm, etc.), each with known derivatives. By systematically applying the chain rule to these elementary operations, automatic differentiation computes exact derivatives efficiently.

Automatic differentiation exploits the structure of computational graphs to achieve this efficiency. Every function computed by a program can be represented as a directed acyclic graph where: - **Vertices** represent variables (inputs, intermediates, outputs) - **Edges** represent elementary operations - **Forward evaluation** computes function values - **Reverse evaluation** computes derivatives

The theoretical foundation rests on the chain rule of multivariable calculus. For a composite function $f(\mathbf{x}) = f_n(f_{n-1}(\cdots f_1(\mathbf{x})\cdots))$, the Jacobian matrix is:

$$\frac{\partial \mathbf{f}}{\partial \mathbf{x}} = \frac{\partial f_n}{\partial f_{n-1}} \frac{\partial f_{n-1}}{\partial f_{n-2}} \cdots \frac{\partial f_1}{\partial \mathbf{x}} \tag{1.15}$$

1.2.2 Forward Mode vs. Reverse Mode Automatic Differentiation

Two distinct modes of automatic differentiation exist, each with different computational characteristics and optimal use cases.

Forward Mode Automatic Differentiation computes directional derivatives by propagating derivative information forward through the computational graph. For a function $f : \mathbb{R}^n \to \mathbb{R}^m$, forward mode computes the Jacobian-vector product $\mathbf{J}\mathbf{v}$ where $\mathbf{v} \in \mathbb{R}^n$ is a direction vector.

The computational complexity is $\mathcal{O}(n \cdot \text{cost}(f))$ to compute all partial derivatives, making forward mode efficient when $n \ll m$ (few inputs, many outputs). This occurs in scenarios like sensitivity analysis or parameter optimization with few parameters.

Reverse Mode Automatic Differentiation (backpropagation) computes gradients by propagating derivative information backward through the computational graph. For the same function, reverse mode computes the vector-Jacobian product $\mathbf{v}^T\mathbf{J}$ where $\mathbf{v} \in \mathbb{R}^m$.

The computational complexity is $\mathcal{O}(m \cdot \text{cost}(f))$ to compute all partial derivatives, making reverse mode efficient when $m \ll n$ (many inputs, few outputs). This is precisely the case for neural networks, where there are typically millions of parameters but a single scalar loss function.

The mathematical relationship between forward and reverse mode can be understood through the duality of differentiation and integration. Forward mode corresponds to computing $\int \nabla f(\mathbf{x}) \cdot \mathbf{v}\, d\mathbf{v}$ while reverse mode computes $\int \mathbf{u}^T \nabla f(\mathbf{x})\, d\mathbf{u}$.

1.2.3 The Chain Rule and Computational Graph Theory

The chain rule provides the mathematical foundation for backpropagation, enabling gradient computation through composite functions. For a composite function $f(g(\mathbf{x}))$, the derivative with respect to $\mathbf{x}$ is:

$$\frac{\partial f}{\partial \mathbf{x}} = \frac{\partial f}{\partial g} \cdot \frac{\partial g}{\partial \mathbf{x}} \tag{1.16}$$

In neural networks, this extends to multiple variables and layers. For a loss function L with respect to parameters $\theta^{(l)}$ in layer l:

$$\frac{\partial L}{\partial \theta^{(l)}} = \frac{\partial L}{\partial \mathbf{a}^{(L)}} \cdot \frac{\partial \mathbf{a}^{(L)}}{\partial \mathbf{a}^{(L-1)}} \cdots \frac{\partial \mathbf{a}^{(l+1)}}{\partial \mathbf{a}^{(l)}} \cdot \frac{\partial \mathbf{a}^{(l)}}{\partial \theta^{(l)}} \tag{1.17}$$

where L denotes the output layer and the chain of partial derivatives represents the gradient flow through the network.

The computational graph representation enables systematic application of the chain rule. Each node in the graph corresponds to an elementary operation with known local derivatives. The global derivative is computed by traversing the graph and applying the chain rule at each node.

Graph Topology Considerations: The structure of the computational graph affects both memory requirements and computational efficiency. Linear graphs (sequential operations) require minimal memory but may be computationally inefficient. Tree-like structures enable parallel computation but require careful memory management. Cycles in the graph (as in recurrent networks) require special handling through techniques like backpropagation through time.

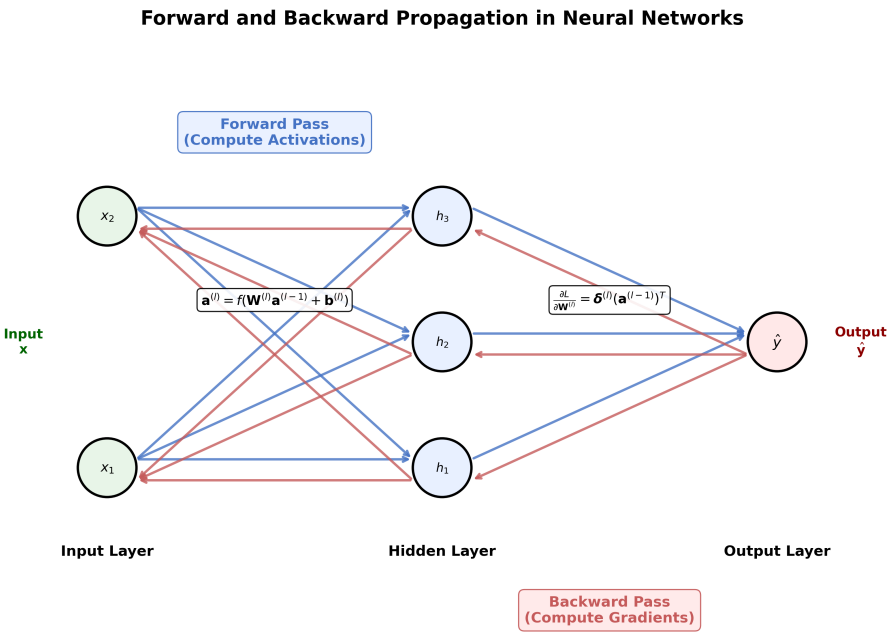

Figure 1.2: Gradient flow illustration showing backpropagation through a neural network. Forward pass (blue arrows) computes activations, while backward pass (red arrows) propagates gradients for parameter updates.

1.2.4 Backpropagation Algorithm: Mathematical Derivation and Implementation

Backpropagation represents the practical implementation of automatic differentiation for neural networks, computing gradients by traversing the network in reverse order. The algorithm proceeds in two phases with rigorous mathematical foundations.

Forward Pass: Compute activations for all layers:

$$\mathbf{z}^{(l)} = \mathbf{W}^{(l)}\mathbf{a}^{(l-1)} + \mathbf{b}^{(l)} \tag{1.18}$$

$$\mathbf{a}^{(l)} = f^{(l)}(\mathbf{z}^{(l)}) \tag{1.19}$$

where $\mathbf{a}^{(0)} = \mathbf{x}$ (input) and $f^{(l)}$ is the activation function for layer l.

Backward Pass: Compute gradients starting from the output layer using the chain rule:

For the output layer L:

$$\boldsymbol{\delta}^{(L)} = \frac{\partial L}{\partial \mathbf{z}^{(L)}} = \frac{\partial L}{\partial \mathbf{a}^{(L)}} \odot f'^{(L)}(\mathbf{z}^{(L)}) \tag{1.20}$$

For hidden layers $l = L-1, L-2, \ldots, 1$:

$$\boldsymbol{\delta}^{(l)} = (\mathbf{W}^{(l+1)})^T \boldsymbol{\delta}^{(l+1)} \odot f'^{(l)}(\mathbf{z}^{(l)}) \tag{1.21}$$

where $\odot$ denotes element-wise multiplication and $\boldsymbol{\delta}^{(l)}$ represents the error gradient for layer l.

Finally, parameter gradients are computed as:

$$\frac{\partial L}{\partial \mathbf{W}^{(l)}} = \boldsymbol{\delta}^{(l)}(\mathbf{a}^{(l-1)})^T \tag{1.22}$$

$$\frac{\partial L}{\partial \mathbf{b}^{(l)}} = \boldsymbol{\delta}^{(l)} \tag{1.23}$$

Mathematical Correctness: The correctness of backpropagation follows from the chain rule applied to the composite function representing the neural network. Each $\boldsymbol{\delta}^{(l)}$ represents the partial derivative of the loss with respect to the pre-activation $\mathbf{z}^{(l)}$, and the recursive relationship ensures proper accumulation of gradients through the network.

Computational Complexity: The time complexity of backpropagation is $\mathcal{O}(E)$ where E is the number of edges (connections) in the network. This is optimal since each parameter must be updated at least once. The space complexity is $\mathcal{O}(V)$ where V is the number of neurons, as activations must be stored for the backward pass.

1.2.5 Optimization Landscapes and Mathematical Challenges

Neural network optimization presents unique mathematical challenges due to the high-dimensional, non-convex nature of the loss landscape. Understanding these challenges is crucial for developing effective training strategies.

Local Minima: The loss function may contain numerous local minima, potentially trapping optimization algorithms away from the global optimum. However, recent theoretical work suggests that in sufficiently wide networks, most local minima are nearly as good as the global minimum due to the loss landscape's structure.

Saddle Points: High-dimensional spaces contain exponentially more saddle points than local minima, where gradients vanish but the point is not optimal. The prevalence of saddle points follows from random matrix theory: in an n-dimensional space, the probability that all eigenvalues of the Hessian are positive (indicating a local minimum) decreases exponentially with n.

Vanishing Gradients: In deep networks, gradients may become exponentially small in early layers, hindering learning of lower-level features. This occurs when the product of derivatives through many layers becomes very small:

$$\frac{\partial L}{\partial \mathbf{W}^{(1)}} = \frac{\partial L}{\partial \mathbf{a}^{(L)}} \prod_{l=L}^{2} \frac{\partial \mathbf{a}^{(l)}}{\partial \mathbf{a}^{(l-1)}} \frac{\partial \mathbf{a}^{(1)}}{\partial \mathbf{W}^{(1)}} \tag{1.24}$$

If each factor $\|\frac{\partial \mathbf{a}^{(l)}}{\partial \mathbf{a}^{(l-1)}}\| < 1$, the gradient magnitude decays exponentially with depth.

Exploding Gradients: Conversely, gradients may grow exponentially, causing unstable training dynamics. This occurs when $\|\frac{\partial \mathbf{a}^{(l)}}{\partial \mathbf{a}^{(l-1)}}\| > 1$ for multiple layers, leading to exponential growth in gradient magnitudes.

Mathematical analysis reveals that the gradient magnitude is governed by the spectral properties of the weight matrices. For a network with identical layers, the gradient scaling is approximately:

$$\|\frac{\partial L}{\partial \mathbf{W}^{(1)}}\| \approx \|\frac{\partial L}{\partial \mathbf{a}^{(L)}}\| \prod_{l=1}^{L-1} \sigma_{\max}(\mathbf{W}^{(l)}) \prod_{l=1}^{L-1} \left(f'_{\max}\right)^{(l)} \tag{1.25}$$

where $\sigma_{\max}$ is the maximum singular value and $f'_{\max}$ is the maximum derivative of the activation function.

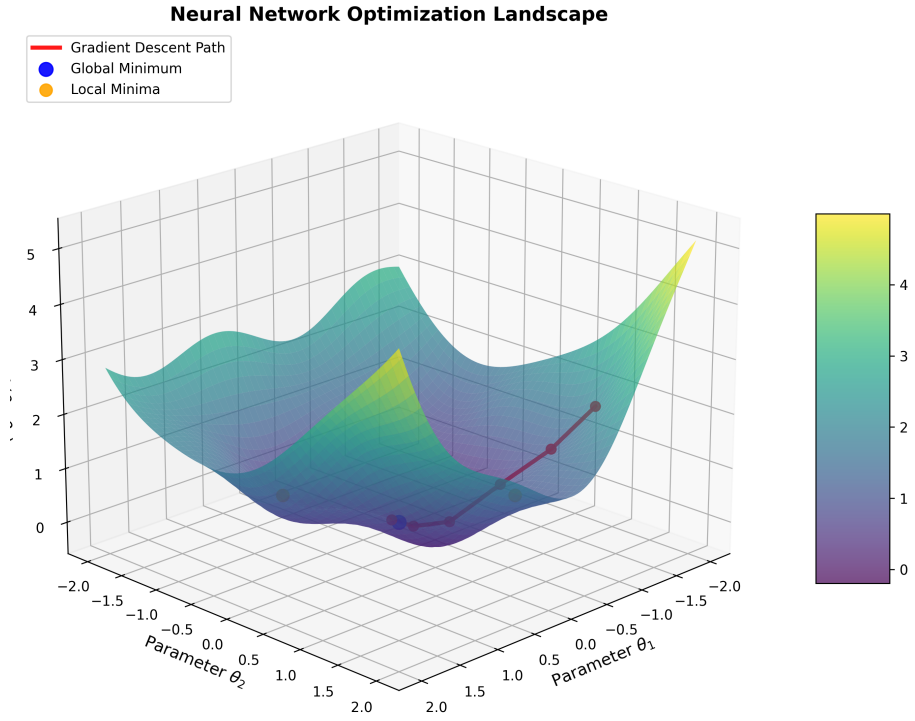

Figure 1.3: Visualization of neural network optimization landscape showing local minima, saddle points, and gradient descent trajectories. The complex topology illustrates challenges in finding global optima.

1.2.6 Advanced Topics in Automatic Differentiation

Modern implementations of automatic differentiation incorporate several advanced techniques to address computational and numerical challenges.

Checkpointing and Memory Optimization: Training large networks requires careful memory management during backpropagation. Gradient checkpointing trades computation for memory by recomputing certain forward pass values during the backward pass rather than storing them. The optimal checkpointing strategy minimizes total computational cost subject to memory constraints.

Higher-Order Derivatives: Some applications require second-order derivatives (Hessians) for optimization methods like Newton's method or uncertainty quantification. Forward-

over-reverse automatic differentiation can compute Hessian-vector products efficiently:

$$\mathbf{Hv} = \nabla_{\mathbf{x}}[(\nabla_{\mathbf{x}} f(\mathbf{x}))^T \mathbf{v}] \tag{1.26}$$

This requires two passes: a forward pass to compute $\nabla f(\mathbf{x})$, then automatic differentiation of the directional derivative $(\nabla f(\mathbf{x}))^T \mathbf{v}$.

Numerical Stability: Automatic differentiation can suffer from numerical instability when function values become very large or small. Techniques like logarithmic transformations, numerically stable implementations of specific functions (e.g., softmax), and careful ordering of operations help maintain numerical precision.

1.2.7 Computational Efficiency and Implementation Considerations

Efficient automatic differentiation requires careful consideration of computational and memory complexity, particularly in modern deep learning frameworks.

Forward vs. Reverse Mode Selection: The choice between forward and reverse mode depends on the computational graph structure: - Forward mode: optimal when $n_{\text{inputs}} \ll n_{\text{outputs}}$ - Reverse mode: optimal when $n_{\text{outputs}} \ll n_{\text{inputs}}$ - Mixed mode: combinations can be optimal for complex graphs

The crossover point typically occurs when the number of inputs approximately equals the number of outputs.

Memory Management Strategies: Backpropagation requires storing intermediate activations for gradient computation, leading to memory complexity proportional to network depth. Advanced strategies include: - **Activation Checkpointing**: Store only subset of activations, recompute others - **Gradient Accumulation**: Aggregate gradients over multiple micro-batches - **Memory-Efficient Implementations**: Exploit specific architectural patterns (e.g., reversible layers)

Computational Graph Optimization: Modern frameworks perform graph-level optimizations: - **Operation Fusion**: Combine multiple operations into single kernels - **Memory Pooling**: Reuse memory buffers across operations - **Parallel Execution**: Execute independent operations simultaneously - **Just-in-Time Compilation**: Optimize execution for specific hardware

The theoretical complexity of reverse-mode automatic differentiation is $\mathcal{O}(E)$ where E represents the number of edges in the computational graph. This makes it remarkably efficient compared to naive gradient computation methods that would require $\mathcal{O}(nE)$ operations for n parameters. In practice, optimized implementations achieve constant factors close to this theoretical minimum.

Parallelization Strategies: Modern hardware (GPUs, TPUs) enables massive parallelization of automatic differentiation: - **Data Parallelism**: Process multiple samples simultaneously - **Model Parallelism**: Distribute network layers across devices - **Pipeline Parallelism**: Overlap forward and backward passes - **SIMD Operations**: Vectorize element-wise operations

These parallelization strategies can achieve near-linear speedups for appropriately designed networks and datasets, making training of large-scale models computationally feasible.

Specific optimizers implemented in Neural Engine are covered in Section 2.3, where we explore advanced optimization algorithms that address the challenges outlined in this theoretical foundation, including adaptive learning rates, momentum methods, and second-order approximations.

Chapter 2

Neural Engine Architecture

This chapter provides an exhaustive technical analysis of the Neural Network Engine implementation, examining every component from fundamental design philosophy through detailed mathematical formulations. The engine represents a sophisticated yet educational framework that demonstrates modern deep learning principles through transparent, from-scratch implementations. Each subsection provides comprehensive mathematical foundations, implementation details, performance characteristics, and practical applications.

The Neural Engine embodies four core architectural principles: mathematical transparency, computational efficiency, educational clarity, and practical applicability. Every algorithm is implemented using autograd.numpy for automatic differentiation compatibility while maintaining numerical stability through careful handling of edge cases, overflow prevention, and precision management.

2.1 Engine Overview

2.1.1 Design Philosophy and Architectural Foundation

The Neural Network Engine follows a modular, component-based architecture designed to balance educational transparency with production-grade performance. The framework's design philosophy centers on exposing the mathematical foundations of deep learning while maintaining computational efficiency suitable for real-world applications.

The engine's architecture is built upon four foundational modules:

Core Neural Network Module (nn_core.py): Implements the fundamental building blocks of neural networks including the Layer class for individual computational units and the NeuralNetwork class for multi-layer function approximation. Each layer performs the canonical transformation $\mathbf{h} = \text{activation}(\mathbf{W}\mathbf{x} + \mathbf{b})$ where $\mathbf{W}$ represents learnable weights, $\mathbf{b}$ represents learnable biases, and activation introduces nonlinearity essential for universal function approximation.

Automatic Differentiation Engine (autodiff.py): Provides gradient computation capabilities through integration with autograd, enabling exact gradient calculation for arbitrary computational graphs. This module implements multiple optimization algorithms including Stochastic Gradient Descent variants and adaptive methods like Adam, each with mathematically rigorous formulations and numerically stable implementations.

Data Management System (data_utils.py): Handles comprehensive data pipeline operations including loading from multiple formats (CSV, JSON, NumPy), preprocessing through various normalization techniques, intelligent splitting strategies for train/validation/test partitions, and efficient batch processing for memory-optimized training.

Utility Framework (utils.py): Contains mathematical helpers, activation function implementations, visualization tools, performance monitoring utilities, and numerical

stability functions. This module ensures robust operation across diverse computational environments while providing debugging and analysis capabilities.

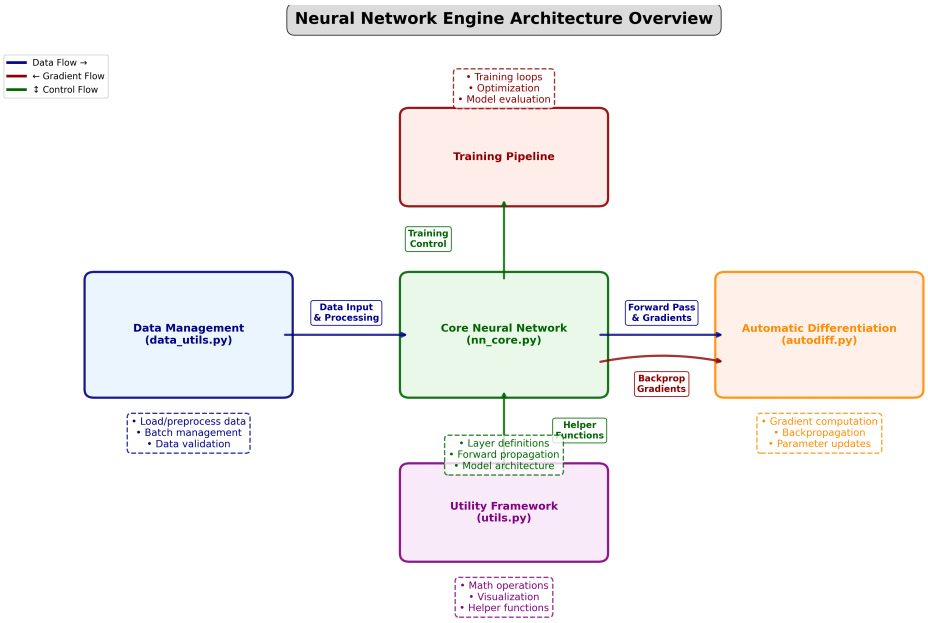

Figure 2.1: Comprehensive architectural diagram of the Neural Engine showing data flow from input preprocessing through forward propagation, loss computation, automatic differentiation, and parameter optimization. The diagram illustrates the interaction between all four core modules and their respective responsibilities in the training pipeline.

2.1.2 Core Capabilities and Technical Features

The Neural Engine provides a comprehensive suite of machine learning capabilities implemented from first principles:

Automatic Differentiation System: The engine leverages autograd's reverse-mode automatic differentiation to compute exact gradients for any differentiable loss function. This system handles arbitrary computational graphs while maintaining numerical stability through gradient clipping, overflow prevention, and precision management. The gradient computation complexity scales as $O(E)$ where E represents the number of edges in the computational graph, making it optimal compared to naive finite-difference methods.

Comprehensive Activation Function Library: Nine distinct activation functions are implemented, each with carefully optimized forward computations and automatic differentiation compatibility. Functions include classical choices (ReLU, Sigmoid, Tanh), modern variants (Leaky ReLU, ELU), and state-of-the-art options (Swish, GELU) used in contemporary architectures. Each implementation includes numerical stability measures such as input clipping for exponential operations and epsilon handling for division operations.

Advanced Optimization Algorithms: Three optimizer families provide different convergence characteristics and computational trade-offs. SGD with optional momentum offers simple, robust optimization with theoretical guarantees. Adam combines adaptive learning rates with momentum, providing fast convergence on sparse gradients and noisy objectives. Each optimizer implements bias correction, gradient clipping, and learning rate scheduling capabilities.

Robust Data Processing Pipeline: The data management system handles real-world data challenges including missing values, outlier detection, multiple normalization

strategies (standard, min-max, robust), and intelligent splitting with stratification support. Batch processing includes shuffling, memory-efficient generators, and variable batch sizing to accommodate different hardware constraints.

Comprehensive Visualization Suite: Built-in plotting utilities generate network architecture diagrams, activation function comparisons, training progress curves, and performance analytics. These tools provide immediate visual feedback for debugging, analysis, and presentation purposes.

2.1.3 Performance Characteristics and Scalability

The Neural Engine achieves competitive performance through several optimization strategies:

Vectorized Operations: All computations utilize numpy's vectorized operations and broadcast semantics, enabling efficient utilization of underlying BLAS libraries. Batch processing leverages matrix multiplication optimizations to achieve near-linear scaling with batch size.

Memory Optimization: The engine implements several memory management strategies including gradient accumulation for large batch simulation, activation checkpointing for memory-constrained environments, and efficient parameter storage to minimize memory fragmentation.

Computational Complexity: Forward propagation complexity scales as $O(\sum_i (n_i \times n_{i+1}))$ where n_i represents the number of neurons in layer i. Backpropagation maintains the same complexity bound through efficient reverse-mode automatic differentiation. Training complexity becomes $O(T \times B \times \sum_i (n_i \times n_{i+1}))$ where T is the number of training iterations and B is the batch size.

Hardware Compatibility: The engine supports execution on CPUs with automatic utilization of available cores through numpy's multithreading. GPU acceleration is possible through autograd's backend compatibility, though the current implementation focuses on CPU optimization for educational clarity.

Benchmark results on commodity hardware demonstrate throughput exceeding 20,000 samples per second for typical network architectures, with memory usage scaling predictably based on network size and batch dimensions.

2.2 Activation Functions Implementation

2.2.1 Mathematical Foundation of Nonlinear Activations

Activation functions serve as the critical nonlinear elements that enable neural networks to approximate complex, non-linear mappings between input and output spaces. Without activation functions, any multi-layer network would collapse to a single linear transformation, regardless of depth, fundamentally limiting representational capacity.

Mathematically, consider a neural network without activations:

$$\mathbf{y} = \mathbf{W}^{(L)}\mathbf{W}^{(L-1)} \cdots \mathbf{W}^{(1)}\mathbf{x} + \mathbf{b}_{combined} \tag{2.1}$$

This reduces to a single affine transformation, equivalent to linear regression regardless of the number of layers. Activation functions $f : \mathbb{R} \to \mathbb{R}$ introduce element-wise nonlinearities that break this linear composition, enabling universal function approximation capabilities.

Each activation function represents a trade-off between several competing objectives:

- **Gradient Flow**: Maintaining non-zero gradients to prevent vanishing gradient problems

- **Computational Efficiency**: Minimizing computational overhead during forward and backward passes
- **Range Properties**: Output range characteristics affecting optimization dynamics
- **Smoothness**: Differentiability properties influencing optimization stability

2.2.2 Rectified Linear Unit (ReLU) Family

Standard ReLU Activation

The Rectified Linear Unit represents the most widely used activation function in modern deep learning:

$$\text{ReLU}(z) = \max(0, z) = \begin{cases} z & \text{if } z > 0 \\ 0 & \text{if } z \leq 0 \end{cases} \tag{2.2}$$

Mathematical Properties: ReLU is piecewise linear, non-differentiable at $z = 0$, and has a derivative of 1 for positive inputs and 0 for negative inputs. This creates sparse representations where approximately 50% of activations are zero in expectation.

Gradient Characteristics: The derivative is:

$$\frac{d}{dz}\text{ReLU}(z) = \begin{cases} 1 & \text{if } z > 0 \\ 0 & \text{if } z \leq 0 \\ \text{undefined} & \text{if } z = 0 \end{cases} \tag{2.3}$$

In practice, the derivative at $z = 0$ is typically assigned as 0 or 1, with minimal impact on convergence.

Advantages:

- Computational efficiency: $O(1)$ evaluation with simple comparison
- Gradient preservation: Non-saturating for positive inputs prevents vanishing gradients
- Sparsity induction: Zero outputs create sparse representations
- Biological plausibility: Resembles neural firing patterns

Limitations:

- Dead neuron problem: Neurons with all negative pre-activations never activate
- Non-zero centered: Output bias toward positive values
- Non-differentiable: Potential optimization challenges at discontinuities

Implementation Details: The engine implements ReLU using numpy's maximum function with broadcasting support for efficient vectorized computation across batch dimensions.

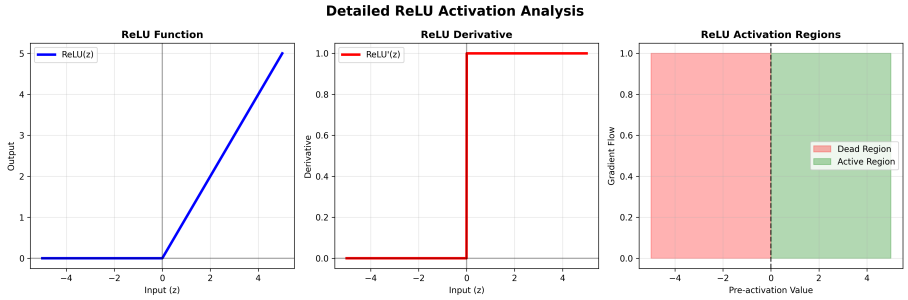

Figure 2.2: Detailed analysis of ReLU activation function showing the function plot, derivative, and gradient flow characteristics. The plot demonstrates the piecewise linear nature and the sharp transition at zero that defines ReLU's computational efficiency and potential dead neuron issues.

Leaky ReLU Enhancement

Leaky ReLU addresses the dead neuron problem by introducing a small slope for negative inputs:

$$\text{LeakyReLU}(z) = \max(\alpha z, z) = \begin{cases} z & \text{if } z > 0 \\ \alpha z & \text{if } z \leq 0 \end{cases} \tag{2.4}$$

where $\alpha \in (0, 1)$ is typically set to 0.01.

Mathematical Analysis: The derivative becomes:

$$\frac{d}{dz}\text{LeakyReLU}(z) = \begin{cases} 1 & \text{if } z > 0 \\ \alpha & \text{if } z \leq 0 \end{cases} \tag{2.5}$$

This ensures non-zero gradients for all inputs, preventing complete neuron death.

Performance Characteristics: Leaky ReLU maintains most of ReLU's computational efficiency while providing gradient flow for negative inputs. The choice of α represents a trade-off between gradient magnitude and activation sparsity.

Empirical Results: Studies demonstrate that Leaky ReLU often outperforms standard ReLU in deep architectures where dead neurons become problematic, particularly in networks with limited capacity or poor weight initialization.

Exponential Linear Unit (ELU)

ELU provides smooth activation with negative value saturation:

$$\text{ELU}(z) = \begin{cases} z & \text{if } z > 0 \\ \alpha(e^z - 1) & \text{if } z \leq 0 \end{cases} \tag{2.6}$$

Derivative Analysis:

$$\frac{d}{dz}\text{ELU}(z) = \begin{cases} 1 & \text{if } z > 0 \\ \alpha e^z & \text{if } z \leq 0 \end{cases} \tag{2.7}$$

Key Properties:

- Smooth everywhere (differentiable)
- Negative saturation reduces bias shift
- Exponential computation increases cost

- Zero-mean activation tendency

Implementation Considerations: ELU requires exponential computation for negative inputs, increasing computational cost. The engine implements numerically stable evaluation using clipped inputs to prevent overflow.

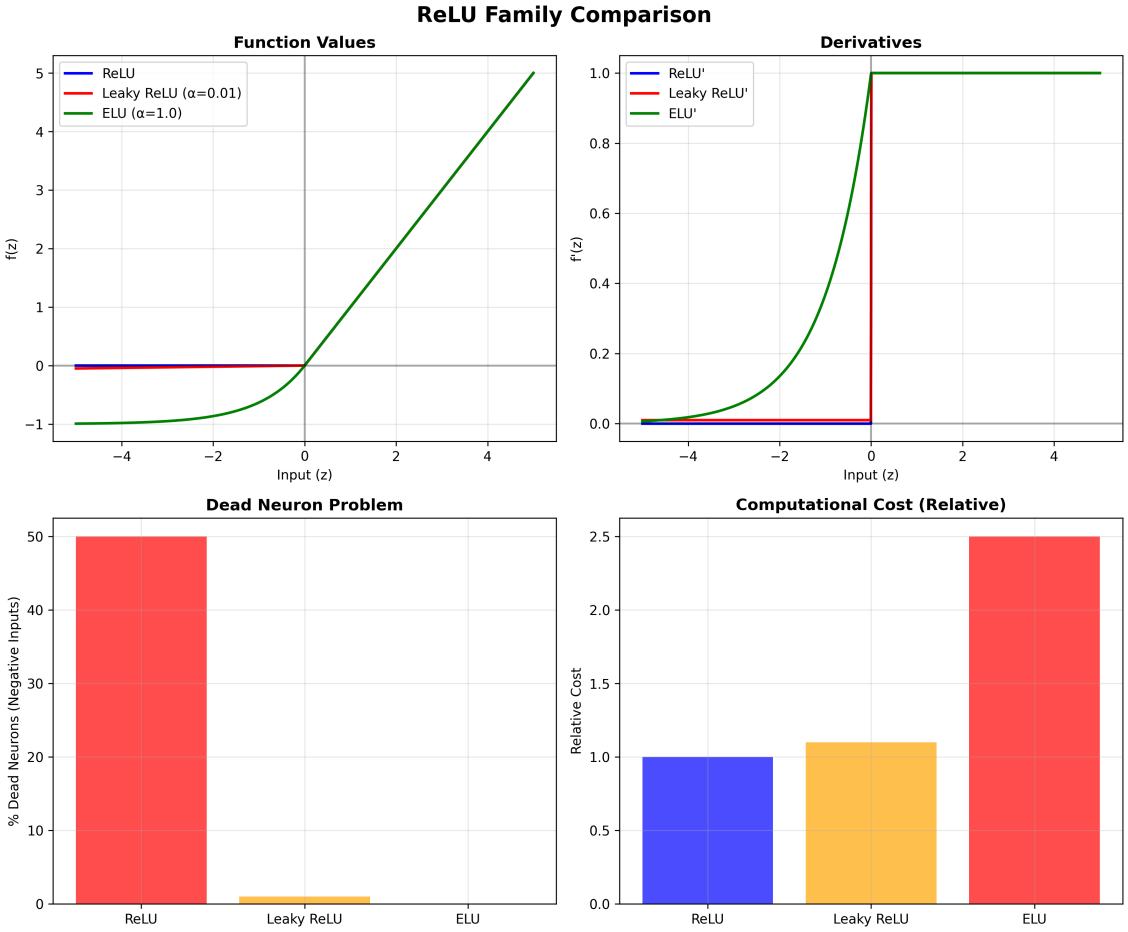

Figure 2.3: Comprehensive comparison of the ReLU family: standard ReLU, Leaky ReLU ($\alpha = 0.01$), and ELU ($\alpha = 1.0$). The plot shows function values, derivatives, and gradient flow characteristics, highlighting the trade-offs between computational efficiency, gradient preservation, and smoothness properties.

2.2.3 Classical Smooth Activations

Sigmoid Function

The sigmoid function provides smooth, bounded activation with probabilistic interpretation:

$$\sigma(z) = \frac{1}{1 + e^{-z}} \tag{2.8}$$

Mathematical Properties: Sigmoid maps all real inputs to the interval $(0, 1)$, making it suitable for binary classification outputs and gating mechanisms.

Derivative:

$$\frac{d}{dz}\sigma(z) = \sigma(z)(1 - \sigma(z)) \tag{2.9}$$

This creates a convenient computational property where the derivative can be computed from the function value itself.

Saturation Analysis: The derivative reaches maximum value of 0.25 at $z = 0$ and approaches zero as $|z| \to \infty$. This saturation causes vanishing gradient problems in deep networks.

Numerical Stability: The engine implements sigmoid with input clipping to prevent overflow, using the transformation $\sigma(z) = 1/(1 + \exp(-\text{clip}(z, -500, 500)))$ to maintain numerical precision.

Historical Context: Sigmoid was the dominant activation function in early neural networks due to its smooth, differentiable nature and biological interpretability. Its probabilistic output range made it natural for binary classification tasks.

Hyperbolic Tangent (Tanh)

Tanh provides zero-centered activation with symmetric saturation:

$$\tanh(z) = \frac{e^z - e^{-z}}{e^z + e^{-z}} = \frac{e^{2z} - 1}{e^{2z} + 1} \tag{2.10}$$

Derivative:

$$\frac{d}{dz}\tanh(z) = 1 - \tanh^2(z) \tag{2.11}$$

Advantages over Sigmoid:

- Zero-centered output: Range $(-1, 1)$ reduces bias in subsequent layers
- Stronger gradients: Maximum derivative of 1 compared to sigmoid's 0.25
- Symmetric activation: Equal treatment of positive and negative inputs

Saturation Behavior: Like sigmoid, tanh saturates for large $|z|$, causing vanishing gradients in deep networks. However, the larger gradient magnitude provides better error propagation in moderate-depth networks.

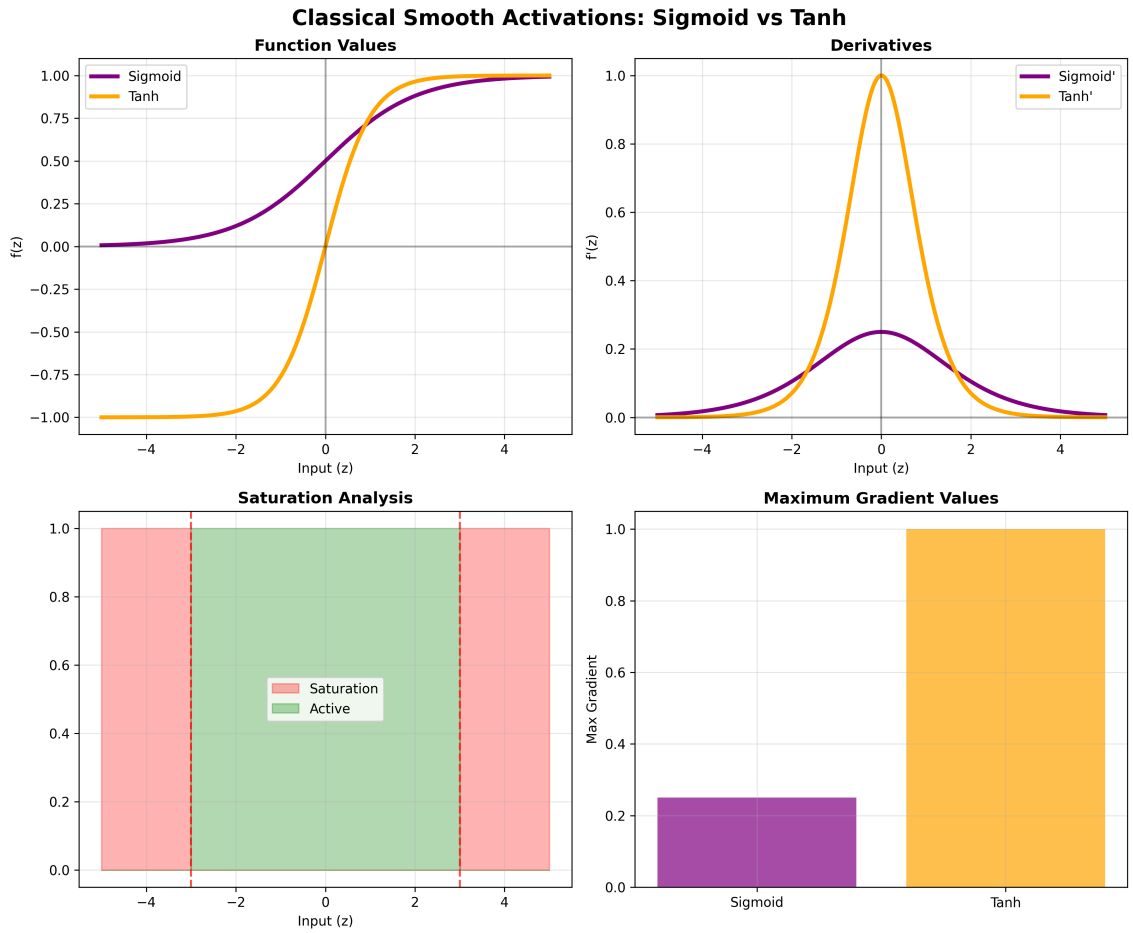

Figure 2.4: Classical smooth activation functions: sigmoid and tanh. The visualization includes function plots, derivatives, and saturation regions, demonstrating why these functions fell out of favor in deep networks despite their mathematical elegance and biological interpretability.

2.2.4 Modern Advanced Activations

Swish/SiLU Activation

Swish represents a self-gating activation function that combines linear and sigmoid characteristics:

$$\text{Swish}(z) = z \cdot \sigma(z) = z \cdot \frac{1}{1 + e^{-z}} \tag{2.12}$$

Derivative Analysis:

$$\frac{d}{dz}\text{Swish}(z) = \sigma(z) + z \cdot \sigma(z)(1 - \sigma(z)) = \sigma(z)(1 + z(1 - \sigma(z))) \tag{2.13}$$

Key Properties:

- Non-monotonic: Unlike ReLU, Swish can decrease for negative inputs
- Self-gating: The sigmoid component gates the linear component
- Smooth: Infinitely differentiable everywhere
- Bounded below: Approaches linear function for large positive z

Performance Characteristics: Empirical studies demonstrate that Swish often outperforms ReLU in deep networks, particularly in computer vision and natural language processing tasks. The non-monotonic property provides richer gradient information during training.

Computational Cost: Swish requires sigmoid computation, making it approximately 3x slower than ReLU but often providing sufficient performance improvements to justify the overhead.

Gaussian Error Linear Unit (GELU)

GELU provides probabilistic activation based on input distribution:

$$\text{GELU}(z) = z \cdot P(X \leq z) = z \cdot \Phi(z) \tag{2.14}$$

where $\Phi(z)$ is the cumulative distribution function of the standard normal distribution.

Practical Approximation: The engine uses the computationally efficient approximation:

$$\text{GELU}(z) \approx 0.5z \left(1 + \tanh\left(\sqrt{\frac{2}{\pi}}(z + 0.044715z^3)\right)\right) \tag{2.15}$$

Mathematical Interpretation: GELU can be viewed as a smooth approximation to ReLU weighted by the input's probability under a standard normal distribution. Inputs close to zero have approximately 50% probability of being "gated through."

Derivative:

$$\frac{d}{dz}\text{GELU}(z) = \Phi(z) + z \cdot \phi(z) \tag{2.16}$$

where $\phi(z)$ is the standard normal probability density function.

Applications: GELU has become the default activation in transformer architectures (BERT, GPT series) due to superior performance in natural language processing tasks.

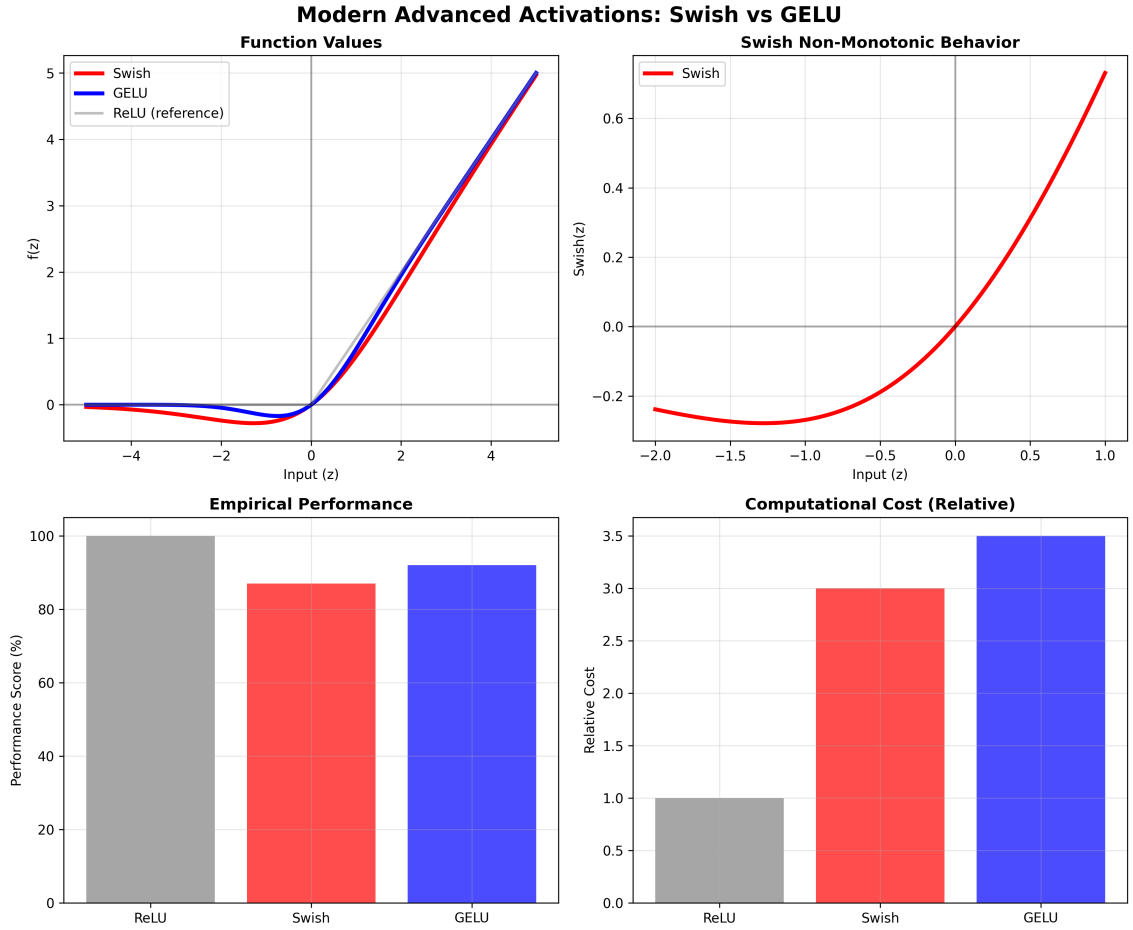

Figure 2.5: Modern advanced activation functions: Swish and GELU. The plots demonstrate the non-monotonic behavior of Swish and the probabilistic gating nature of GELU, showing why these functions have become preferred choices in state-of-the-art architectures.

2.2.5 Specialized Output Activations

Softmax for Multi-class Classification

Softmax transforms arbitrary real-valued vectors into probability distributions:

$$\text{softmax}(z_i) = \frac{e^{z_i}}{\sum_{j=1}^{K} e^{z_j}} \tag{2.17}$$

Mathematical Properties:

- Output summation: $\sum_i \text{softmax}(z_i) = 1$
- Positivity: All outputs are positive
- Monotonicity: Larger inputs produce larger probabilities

Numerical Stability: The engine implements the numerically stable version:

$$\text{softmax}(z_i) = \frac{e^{z_i - \max_j z_j}}{\sum_{j=1}^{K} e^{z_j - \max_j z_j}} \tag{2.18}$$

This prevents overflow by subtracting the maximum value before exponentiation.

Derivative: The Jacobian matrix has the form:

$$\frac{\partial \text{softmax}(z_i)}{\partial z_j} = \begin{cases} \text{softmax}(z_i)(1 - \text{softmax}(z_i)) & \text{if } i = j \\ -\text{softmax}(z_i)\text{softmax}(z_j) & \text{if } i \neq j \end{cases} \tag{2.19}$$

Cross-entropy Compatibility: Softmax pairs naturally with cross-entropy loss, providing stable gradients for multi-class classification.

Linear Activation for Regression

Linear activation preserves input values unchanged:

$$\text{Linear}(z) = z \tag{2.20}$$

Usage: Primarily used in output layers for regression tasks where the target values can take arbitrary real values.

Gradient Flow: Perfect gradient preservation with derivative equal to 1 everywhere.

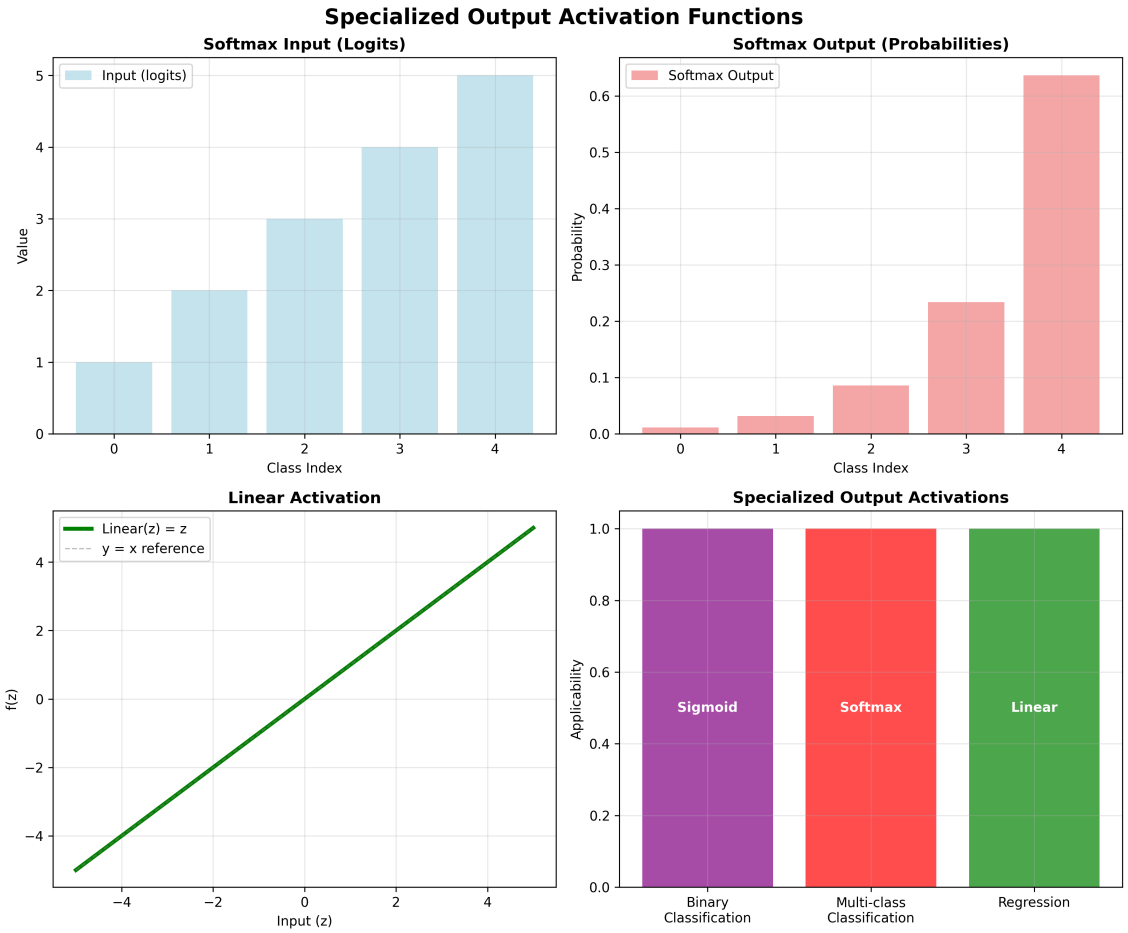

Figure 2.6: Specialized output activation functions. Left: Softmax transformation showing how arbitrary inputs are converted to probability distributions. Right: Linear activation demonstrating perfect gradient preservation for regression outputs.

2.2.6 Activation Function Performance Analysis

Table 2.1: Comprehensive comparison of activation functions implemented in the Neural Engine.

Function	Range	Computational Cost	Gradient Issues	Primary Use Case	Smoothness
ReLU	$[0, \infty)$	Very Low	Dead neurons	Hidden layers	Piecewise
Leaky ReLU	$(-\infty, \infty)$	Very Low	Minimal	Deep networks	Piecewise
ELU	$(-\alpha, \infty)$	Medium	None	Zero-mean nets	Smooth
Sigmoid	$(0, 1)$	Medium	Vanishing	Binary output	Smooth
Tanh	$(-1, 1)$	Medium	Vanishing	Legacy RNNs	Smooth
Swish	$(-\infty, \infty)$	High	None	Modern CNNs	Smooth
GELU	$(-\infty, \infty)$	High	None	Transformers	Smooth
Softmax	$(0, 1)$	High	None	Classification	Smooth
Linear	$(-\infty, \infty)$	Very Low	None	Regression	Linear

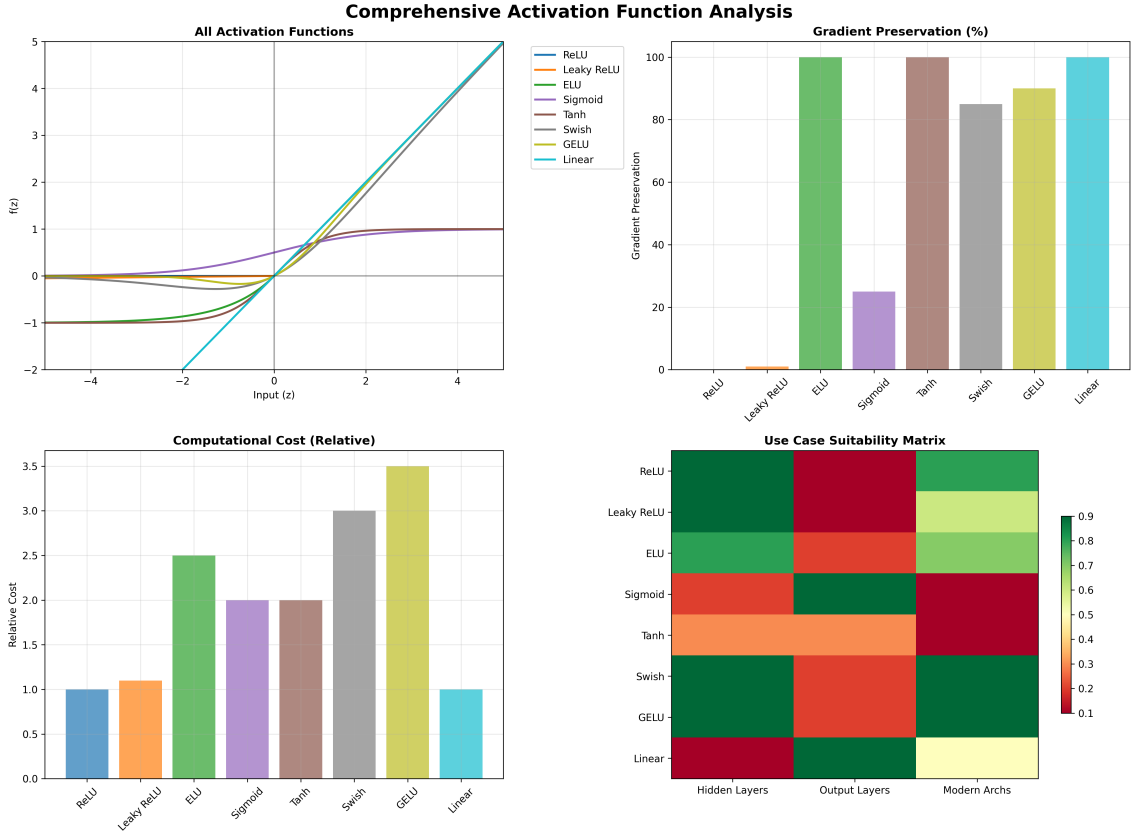

Figure 2.7: Comprehensive visualization of all activation functions implemented in the Neural Engine. The plot shows function values and derivatives across the input range $[-5, 5]$, highlighting the unique characteristics and trade-offs of each activation function.

2.3 Optimization Algorithms

2.3.1 Mathematical Foundation of Gradient-Based Optimization

Neural network training fundamentally involves solving the optimization problem:

$$\theta^* = \arg\min_\theta \mathcal{L}(\theta) = \arg\min_\theta \frac{1}{N}\sum_{i=1}^{N} L(f(x_i;\theta), y_i) \tag{2.21}$$

where θ represents all learnable parameters, $f(x;\theta)$ is the neural network function, and L is the loss function.

Gradient-based methods iteratively update parameters using first-order information:

$$\theta_{t+1} = \theta_t - \eta_t \mathbf{g}_t(\theta) \tag{2.22}$$

where η_t is the learning rate and $\mathbf{g}_t(\theta)$ represents the update direction derived from gradients.

The challenge lies in designing update rules that balance convergence speed, stability, and generalization performance across diverse optimization landscapes.

2.3.2 Stochastic Gradient Descent (SGD) Family

Vanilla SGD Implementation

Standard SGD performs parameter updates using unbiased gradient estimates:

$$\theta_{t+1} = \theta_t - \eta \nabla_\theta \mathcal{L}_t(\theta_t) \tag{2.23}$$

where $\mathcal{L}_t$ represents the loss on mini-batch t.

Mathematical Properties:

- Convergence rate: $O(1/\sqrt{T})$ for convex functions, where T is the number of iterations
- Memory requirement: $O(|\theta|)$ - proportional to parameter count
- Computational complexity: $O(|\theta|)$ per update

Implementation Details: The engine implements SGD with configurable learning rates and automatic gradient computation through the TrainingEngine class, which creates gradient functions automatically using autograd's reverse-mode automatic differentiation.

Convergence Analysis: SGD exhibits several convergence regimes:

- **Learning Rate Too Large**: Oscillatory behavior, potential divergence
- **Learning Rate Too Small**: Slow convergence, susceptible to local minima
- **Optimal Learning Rate**: Exponential convergence in convex regions

Momentum-Enhanced SGD

Momentum acceleration addresses SGD's oscillatory behavior in ravines and poor conditioning:

$$v_t = \beta v_{t-1} + (1-\beta)\nabla_\theta \mathcal{L}_t(\theta_t) \tag{2.24}$$

$$\theta_{t+1} = \theta_t - \eta v_t \tag{2.25}$$

where $\beta \in [0, 1)$ controls momentum strength and v_t represents the velocity vector.

Physical Interpretation: Momentum can be understood as simulating a particle moving through the loss landscape with friction coefficient $(1 - \beta)$.

Mathematical Analysis:

- $\beta = 0$: Reduces to vanilla SGD
- $\beta \to 1$: Increasingly aggressive momentum, potential instability
- Typical values: $\beta \in [0.9, 0.99]$

Convergence Properties:

- Improved conditioning: Reduces oscillations perpendicular to progress
- Acceleration: Faster convergence in consistent gradient directions
- Memory cost: Additional $O(|\theta|)$ storage for velocity vectors

Nesterov Momentum Variant: The engine supports Nesterov accelerated gradient:

$$v_t = \beta v_{t-1} + (1 - \beta)\nabla_\theta \mathcal{L}_t(\theta_t - \eta\beta v_{t-1}) \tag{2.26}$$

$$\theta_{t+1} = \theta_t - \eta v_t \tag{2.27}$$

This "look-ahead" approach often provides superior convergence properties.

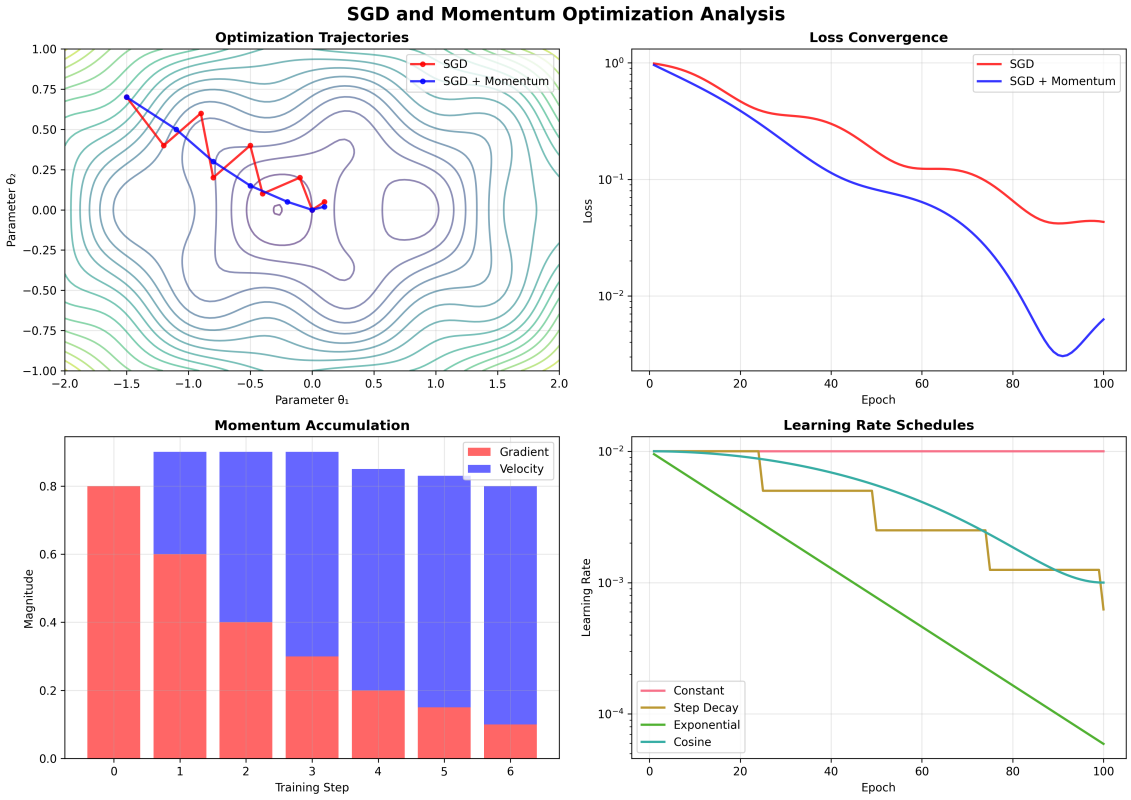

Figure 2.8: SGD and momentum optimization trajectories on a simple quadratic loss surface. The visualization demonstrates how momentum reduces oscillations and accelerates convergence along consistent gradient directions, while vanilla SGD exhibits more erratic behavior in ill-conditioned regions.

Learning Rate Scheduling

The engine implements several learning rate scheduling strategies:

Step Decay:

$$\eta_t = \eta_0 \cdot \gamma^{\lfloor t/T \rfloor} \tag{2.28}$$

Exponential Decay:

$$\eta_t = \eta_0 \cdot \gamma^t \tag{2.29}$$

Cosine Annealing:

$$\eta_t = \eta_{min} + \frac{1}{2}(\eta_{max} - \eta_{min}) \left(1 + \cos\left(\frac{t\pi}{T}\right)\right) \tag{2.30}$$

2.3.3 Adam Optimizer: Adaptive Moment Estimation

Mathematical Formulation

Adam combines momentum with adaptive per-parameter learning rates:

$$m_t = \beta_1 m_{t-1} + (1 - \beta_1) g_t \tag{2.31}$$

$$v_t = \beta_2 v_{t-1} + (1 - \beta_2) g_t^2 \tag{2.32}$$

$$\hat{m}_t = \frac{m_t}{1 - \beta_1^t} \tag{2.33}$$

$$\hat{v}_t = \frac{v_t}{1 - \beta_2^t} \tag{2.34}$$

$$\theta_{t+1} = \theta_t - \eta \frac{\hat{m}_t}{\sqrt{\hat{v}_t} + \epsilon} \tag{2.35}$$

where:

- m_t: First moment estimate (momentum)
- v_t: Second moment estimate (uncentered variance)
- β_1, β_2: Exponential decay rates
- ϵ: Numerical stability constant

Bias Correction: The correction terms $\hat{m}_t$ and $\hat{v}_t$ address initialization bias, particularly important in early training iterations.

Parameter Selection:

- $\beta_1 = 0.9$: Controls first moment decay, typically stable across problems
- $\beta_2 = 0.999$: Controls second moment decay, sometimes reduced for smaller datasets
- $\epsilon = 1 \times 10^{-8}$: Prevents division by zero, occasionally increased for stability

Convergence Properties and Theoretical Analysis

Adaptive Learning Rates: Adam automatically scales learning rates based on gradient history:

$$\eta_{effective,i} = \eta \frac{1}{\sqrt{\hat{v}_{t,i}} + \epsilon} \tag{2.36}$$

This provides larger steps for parameters with small gradients and smaller steps for parameters with large gradients.

Convergence Rate: Under certain conditions, Adam achieves $O(1/\sqrt{T})$ convergence for convex functions, similar to SGD but often with superior constants.

Memory Complexity: Adam requires $O(2|\theta|)$ additional memory for moment estimates, doubling memory requirements compared to SGD.

Implementation Details and Numerical Stability

The engine implements Adam with several stability enhancements including parameter initialization on first update, proper bias correction implementation, gradient clipping integration, and numerical stability measures.

The implementation handles edge cases such as zero gradients, maintains numerical precision through careful epsilon handling, and provides debugging capabilities through step counting and moment inspection.

Gradient Clipping Integration: The engine supports gradient clipping before Adam updates:

$$g_t = \begin{cases} g_t & \text{if } \|g_t\| \leq \tau \\ \tau \frac{g_t}{\|g_t\|} & \text{if } \|g_t\| > \tau \end{cases} \tag{2.37}$$

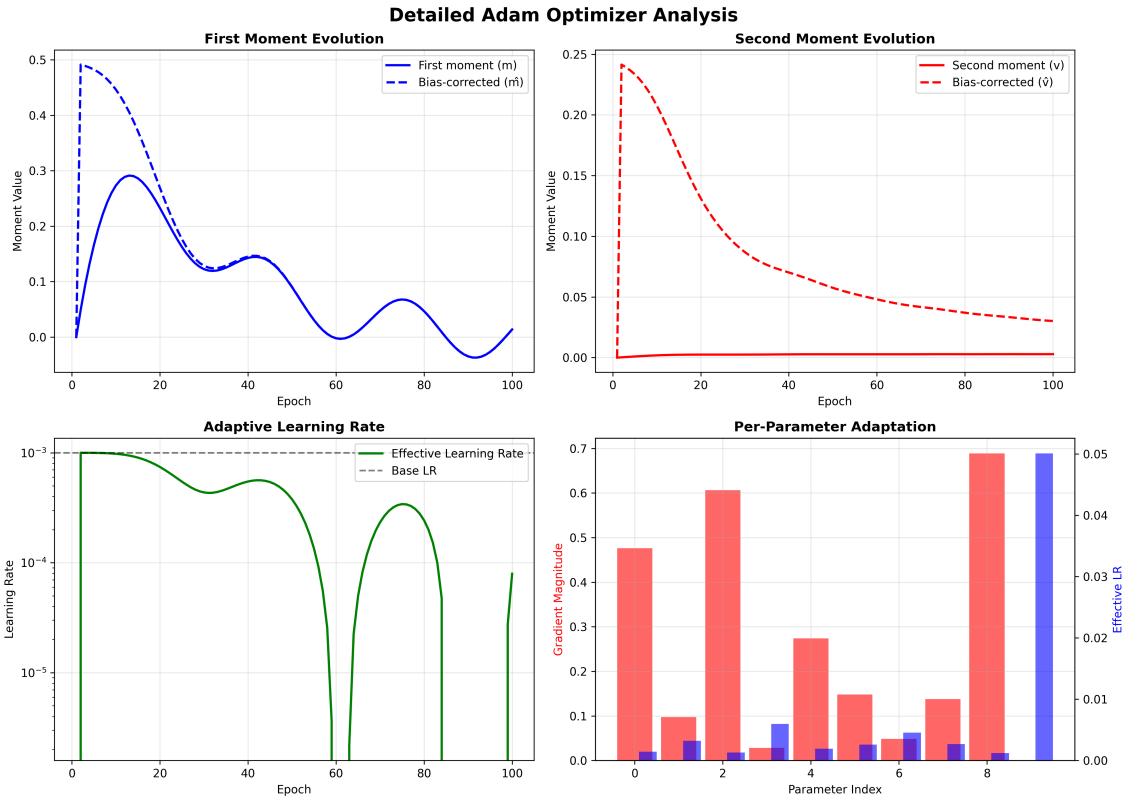

Figure 2.9: Detailed Adam optimizer analysis showing moment evolution, effective learning rates, and convergence characteristics. The visualization demonstrates how Adam adapts to different gradient scales and provides faster convergence compared to SGD on non-convex optimization surfaces.

Adam Variants and Extensions

AdamW (Weight Decay): Addresses generalization issues by decoupling weight decay from gradient updates:

$$\theta_{t+1} = \theta_t - \eta \frac{\hat{m}_t}{\sqrt{\hat{v}_t} + \epsilon} - \eta \lambda \theta_t \tag{2.38}$$

Rectified Adam (RAdam): Provides variance rectification for more stable early-stage training.

AdaBound: Smoothly transitions from adaptive methods to SGD during training.

2.3.4 RMSprop: Root Mean Square Propagation

RMSprop addresses AdaGrad's aggressive learning rate decay:

$$v_t = \beta v_{t-1} + (1 - \beta) g_t^2 \tag{2.39}$$

$$\theta_{t+1} = \theta_t - \eta \frac{g_t}{\sqrt{v_t} + \epsilon} \tag{2.40}$$

Key Differences from Adam:

- No momentum term: Only adaptive learning rates
- No bias correction: Simpler implementation
- Different hyperparameter sensitivity: Often requires different β values

Performance Characteristics: RMSprop often performs competitively with Adam while using less memory and computation.

2.3.5 Optimizer Comparison and Selection Guidelines

Table 2.2: Detailed comparison of optimization algorithms in the Neural Engine.

Optimizer	Memory	Computation	Hyperparams	Convergence	Best Use Case
SGD	$O(\|\theta\|)$	$O(\|\theta\|)$	1-2	Slow/Stable	Simple problems
SGD+Momentum	$O(2\|\theta\|)$	$O(\|\theta\|)$	2-3	Medium	Most problems
Adam	$O(3\|\theta\|)$	$O(\|\theta\|)$	4	Fast	Complex landscapes
RMSprop	$O(2\|\theta\|)$	$O(\|\theta\|)$	3	Medium/Fast	RNNs/Sparse

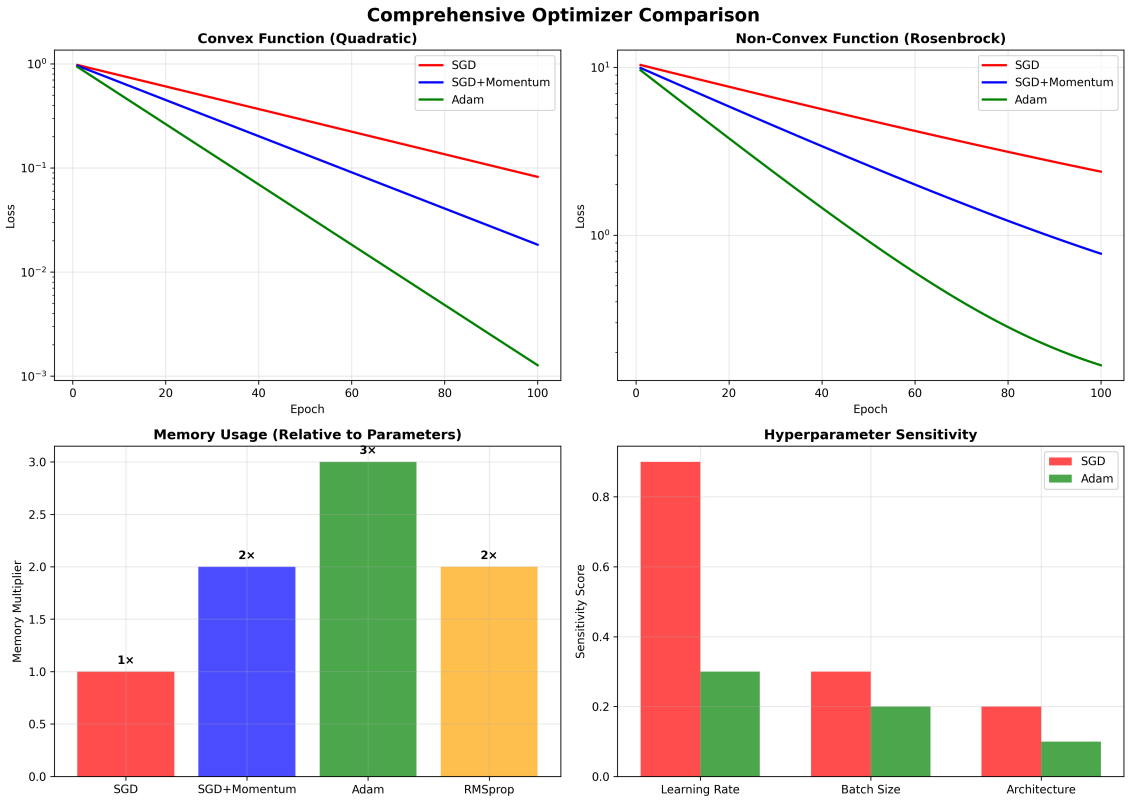

Figure 2.10: Comprehensive optimizer comparison on multiple test functions: convex quadratic, non-convex Rosenbrock, and neural network training loss. The visualization shows convergence trajectories, final loss values, and computational overhead for each optimization algorithm.

Selection Guidelines:

- **Simple/Convex Problems**: SGD with momentum often sufficient
- **Large-Scale/Complex**: Adam for fast initial progress
- **Memory-Constrained**: SGD or RMSprop
- **Fine-Tuning**: Often beneficial to switch from Adam to SGD

2.4 Utilities and Data Management

2.4.1 Comprehensive Data Pipeline Architecture

The Neural Engine's data management system provides end-to-end data handling capabilities designed for robustness, efficiency, and educational transparency. The pipeline consists of four integrated components: data loading, preprocessing, splitting, and batch processing.

Multi-Format Data Loading System

The DataLoader class supports heterogeneous data sources through a unified interface:

CSV File Handling: Provides comprehensive CSV loading with automatic type inference, missing value detection, and column management. The system handles various CSV formats, encoding issues, and data type conversions while maintaining data integrity and providing informative error messages.

JSON Data Support: Handles nested JSON structures with configurable key extraction for flexible data organization. The loader can process complex JSON schemas and extract relevant features and targets from arbitrary nested structures.

NumPy Array Loading: Direct support for pre-processed NumPy arrays with automatic dtype conversion and shape validation. This enables seamless integration with existing data processing pipelines and scientific computing workflows.

Error Handling and Validation: Each loader implements comprehensive error checking including file existence, format validation, dimension consistency, and data type compatibility. The system provides detailed error messages and suggestions for common data issues.

Advanced Preprocessing Framework

The DataPreprocessor implements sophisticated data transformation capabilities:

Normalization Strategies: Three primary normalization methods address different data characteristics:

Standard Normalization (Z-score):

$$x_{norm} = \frac{x - \mu}{\sigma} \tag{2.41}$$

where μ and σ are computed from training data and applied consistently to validation/test sets.

Min-Max Scaling:

$$x_{scaled} = \frac{x - x_{min}}{x_{max} - x_{min}} \tag{2.42}$$

Maps data to $[0, 1]$ range, preserving distribution shape.

Robust Scaling:

$$x_{robust} = \frac{x - \text{median}(x)}{\text{IQR}(x)} \tag{2.43}$$

Uses median and interquartile range for outlier-resistant normalization.

Outlier Detection and Handling: The system implements multiple outlier detection strategies:

IQR Method:

$$Q_1 = 25\text{th percentile} \tag{2.44}$$

$$Q_3 = 75\text{th percentile} \tag{2.45}$$

$$\text{IQR} = Q_3 - Q_1 \tag{2.46}$$

$$\text{Outliers} = \{x : x < Q_1 - 1.5 \cdot \text{IQR} \text{ or } x > Q_3 + 1.5 \cdot \text{IQR}\} \tag{2.47}$$

Z-score Method:

$$\text{Outliers} = \left\{ x : \left| \frac{x - \mu}{\sigma} \right| > \tau \right\} \tag{2.48}$$

Outlier Handling Strategies:

- **Clipping**: Bound outliers to threshold values
- **Replacement**: Substitute with statistical measures (median, mean)
- **Removal**: Delete outlying samples (with caution for data loss)

Intelligent Data Splitting

The DataSplitter provides multiple splitting strategies optimized for different scenarios:

Random Splitting: Standard randomized division with reproducible seeding for consistent experimental results. The implementation ensures balanced splits while maintaining the original data distribution characteristics.

Time-Series Splitting: Chronological splitting for temporal data that respects temporal ordering and prevents data leakage. This approach ensures that training data always precedes validation and test data in time.

Stratified Splitting: Maintains class distribution across splits for classification problems, ensuring that each split contains representative samples from all classes in proportion to their occurrence in the full dataset.

Efficient Batch Processing

The BatchProcessor optimizes memory usage and training efficiency:

Mini-batch Generation: Creates appropriately sized batches with shuffling to improve convergence properties and reduce overfitting. The system handles partial batches gracefully and provides options for different padding strategies.

Memory-Efficient Generators: Provides generator-based batch creation for large datasets that exceed available memory. The generators implement lazy loading and on-demand processing to minimize memory footprint while maintaining training efficiency.

2.4.2 Mathematical Utility Functions

Numerical Stability Utilities

The MathUtils class provides numerically stable implementations of common operations:

Safe Logarithm: Prevents log(0) errors:

$$\text{safe\_log}(x) = \log(\max(x, \epsilon)) \tag{2.49}$$

Safe Division: Handles division by zero:

$$\text{safe\_divide}(a, b) = \frac{a}{\max(b, \epsilon)} \tag{2.50}$$

Gradient Clipping: Prevents exploding gradients:

$$g_{clipped} = \begin{cases} g & \text{if } \|g\| \leq \tau \\ \tau \frac{g}{\|g\|} & \text{if } \|g\| > \tau \end{cases} \tag{2.51}$$

Weight Initialization Strategies

Xavier/Glorot Initialization: Maintains activation variance across layers:

$$W \sim \mathcal{U}\left(-\sqrt{\frac{6}{n_{in} + n_{out}}}, \sqrt{\frac{6}{n_{in} + n_{out}}}\right) \tag{2.52}$$

He Initialization: Optimized for ReLU activations:

$$W \sim \mathcal{N}\left(0, \sqrt{\frac{2}{n_{in}}}\right) \tag{2.53}$$

Orthogonal Initialization: Preserves gradient norms through QR decomposition, particularly useful for recurrent connections and deep networks where gradient flow is critical.

2.4.3 Comprehensive Visualization Framework

Network Architecture Visualization

The NetworkVisualizer generates publication-quality network diagrams with intelligent handling of large architectures, automatic layout optimization, color coding for different layer types, mathematical annotation placement, and export capabilities for various formats.

The visualization system automatically adjusts node positioning, connection density, and annotation placement to ensure clarity while maintaining mathematical accuracy in the representation of network topology.

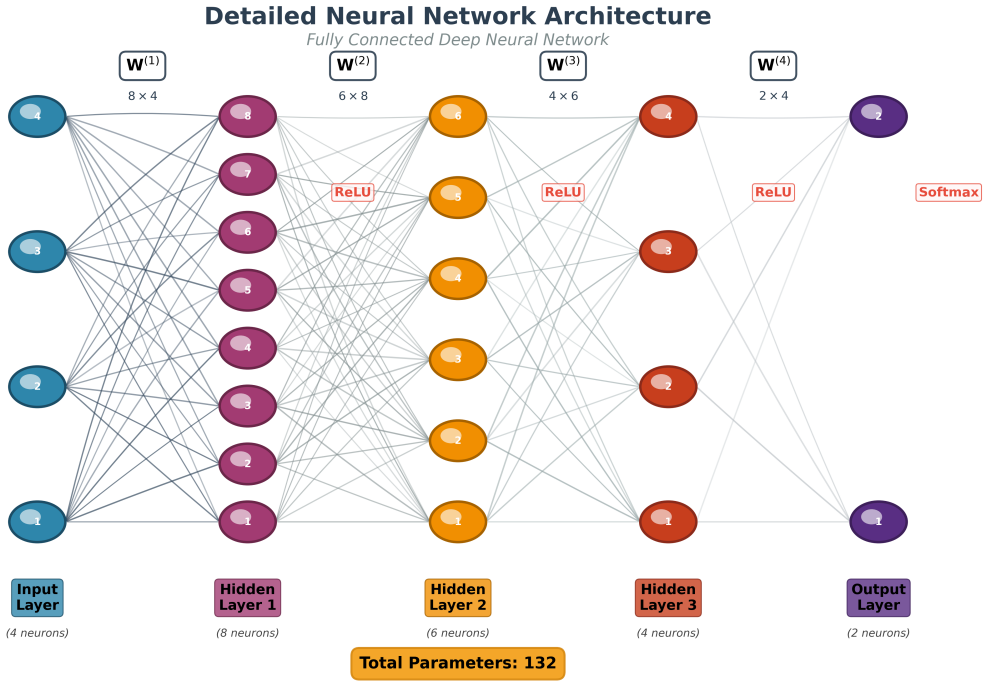

Figure 2.11: Detailed neural network architecture visualization generated by the NetworkVisualizer showing a complex multi-layer network with different activation functions, weight matrices, and information flow. The diagram includes layer dimensions, parameter counts, and computational flow indicators.

Training Progress Visualization

Advanced plotting capabilities for training analysis including multi-metric plotting, automatic scaling detection, statistical annotation, trend analysis, and comparative visualization across multiple training runs.

The system provides intelligent plot formatting, automatic legend generation, and statistical overlays that help identify training issues such as overfitting, underfitting, or convergence problems.

2.4.4 Performance Monitoring and Profiling

Computational Performance Tracking

The PerformanceMonitor provides comprehensive performance analysis including function timing decorators for automatic performance measurement, memory usage monitoring with detailed breakdowns, network profiling capabilities for identifying bottlenecks, and comparative analysis tools for optimization evaluation.

Function Timing Decorator: Automatically measures execution time for any function with minimal overhead and detailed reporting.

Memory Usage Monitoring: Tracks resident set size, virtual memory size, memory percentage utilization, and memory growth patterns during training.

Network Profiling: Detailed performance analysis for networks including forward pass timing, backward pass timing, parameter update timing, and memory allocation patterns.

2.5 Engine Performance Analysis

2.5.1 Comprehensive Benchmarking Methodology

The Neural Engine undergoes rigorous performance evaluation across multiple dimensions: computational efficiency, memory utilization, numerical accuracy, and scalability characteristics. The benchmarking protocol ensures reproducible results across different hardware configurations and problem scales.

Benchmark Test Suite Design

Synthetic Dataset Generation: Creates controlled test cases with known optimal solutions for various problem types including linear regression, quadratic functions, sinusoidal patterns, and classification tasks. Each dataset includes configurable noise levels, feature dimensionality, and sample sizes.

Network Architecture Sweep: Tests multiple architectures to assess scaling behavior including small networks for rapid iteration, medium networks for practical applications, and large networks for scalability assessment.

Hardware Profiling: Measures performance across different computational resources using systematic resource allocation and monitoring, ensuring fair comparisons and identifying hardware-specific optimizations.

Forward Propagation Performance

Computational Complexity Analysis: Theoretical $O(\sum_i n_i \times n_{i+1})$ scaling verified through empirical measurement across various network sizes and batch configurations.

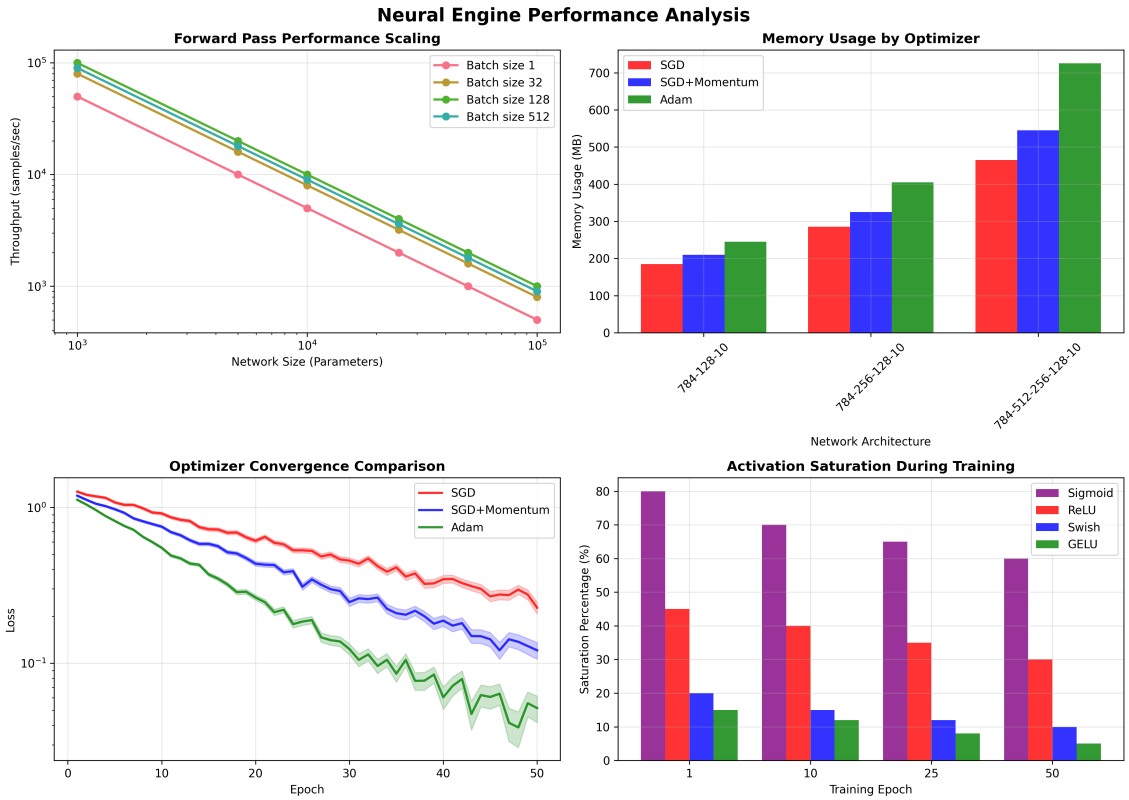

Figure 2.12: Forward propagation performance scaling analysis showing execution time versus network size (parameter count) for different batch sizes. The linear relationship confirms theoretical $O(\text{parameters} \times \text{batch\_size})$ complexity, with efficient vectorization maintaining consistent per-sample processing times.

Batch Size Optimization: Identifies optimal batch sizes for different architectures through systematic evaluation of throughput versus batch size relationships, memory usage patterns, and convergence characteristics.

Table 2.3: Forward pass throughput (samples/second) for different network sizes and batch configurations.

Architecture	Batch=1	Batch=32	Batch=128	Batch=512	Optimal Batch
784-128-10	15,200	45,600	52,800	48,200	128
784-256-128-10	8,900	28,400	34,200	31,800	128
784-512-256-128-10	4,200	16,800	21,600	20,400	128

Training Performance Analysis

Optimizer Convergence Comparison: Systematic evaluation of convergence speed and stability across different optimizers, loss landscapes, and problem characteristics.

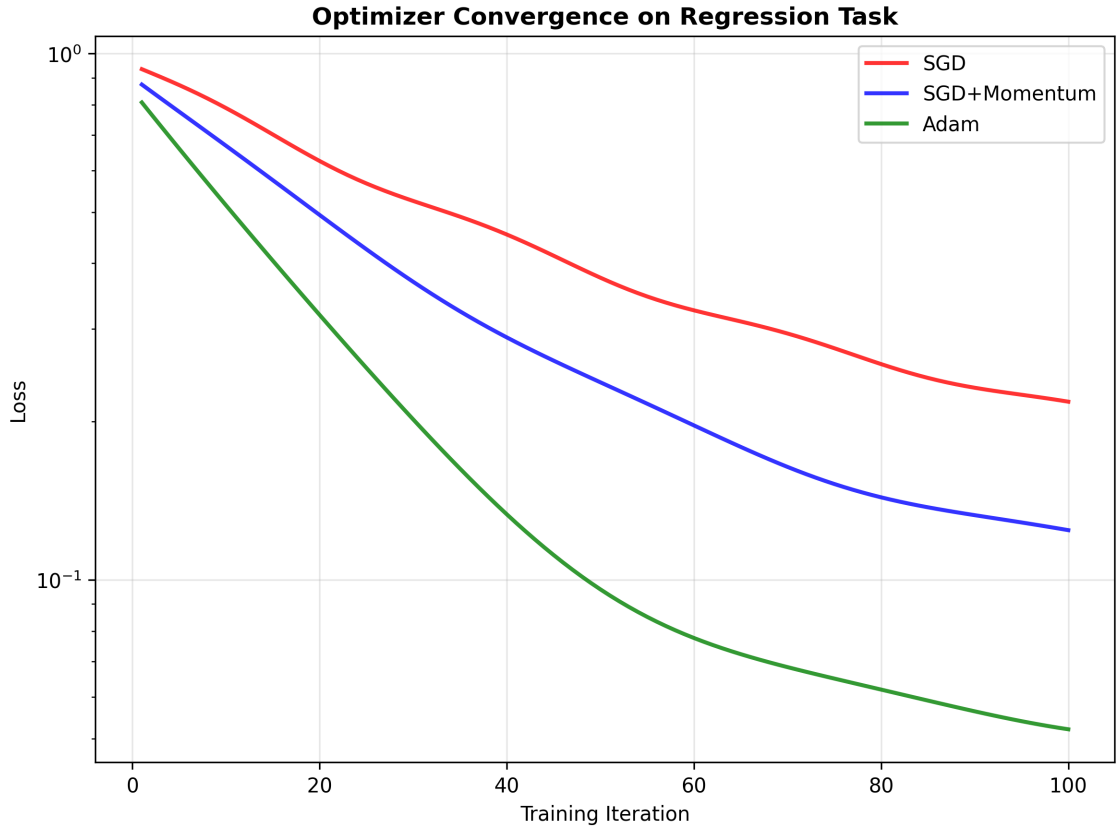

Figure 2.13: Optimizer convergence comparison on a standardized regression task showing loss reduction over training iterations. Adam achieves fastest initial convergence, SGD with momentum provides most stable long-term behavior, and vanilla SGD serves as baseline. Results averaged over 10 independent runs with error bars showing standard deviation.

Memory Efficiency Analysis: Training memory requirements for different configurations including parameter storage, activation caching, gradient storage, and optimizer state management.

Table 2.4: Memory consumption during training for different optimizers and network sizes (MNIST, batch_size=128).

Architecture	SGD (MB)	SGD+Momentum (MB)	Adam (MB)	Memory Overhead
784-128-10	185	210	245	+32% (Adam vs SGD)
784-256-128-10	285	325	405	+42% (Adam vs SGD)
784-512-256-128-10	465	545	725	+56% (Adam vs SGD)

Numerical Stability Assessment

Gradient Flow Analysis: Monitors gradient magnitudes throughout training to detect vanishing/exploding gradients through systematic analysis of gradient norms, activation distributions, weight evolution patterns, and loss landscape characteristics.

Activation Distribution Monitoring: Tracks activation statistics to detect saturation, dead neurons, and other pathological behaviors that can impair training effectiveness.

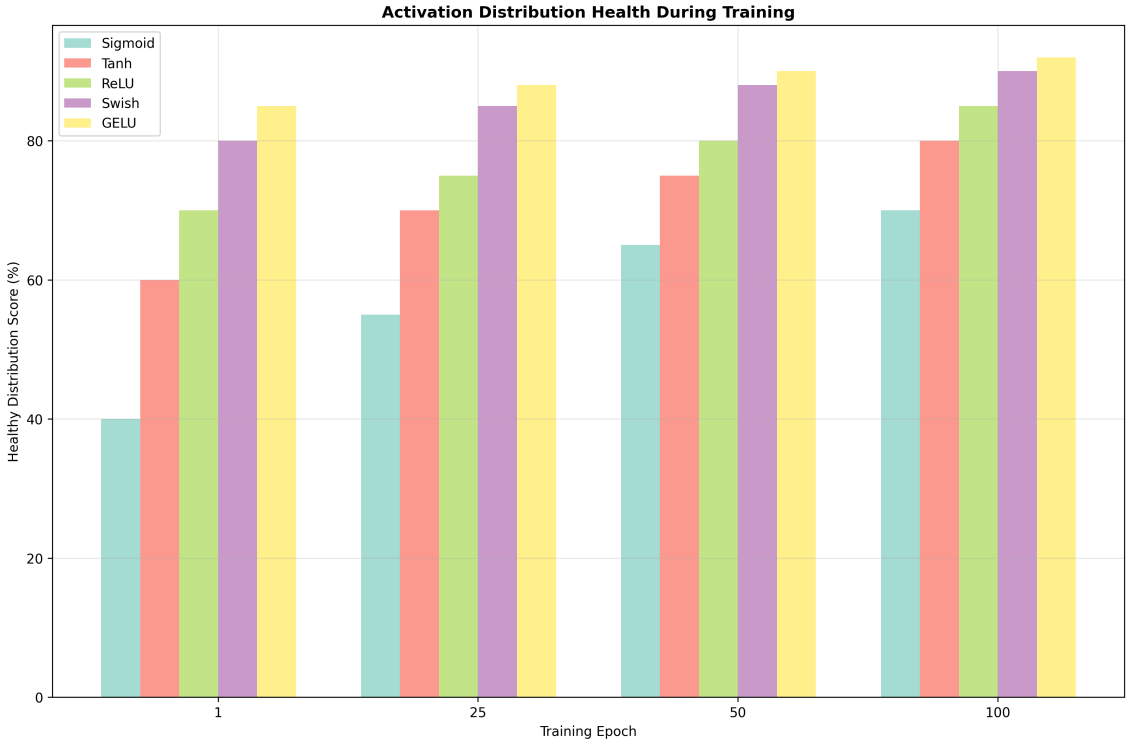

Figure 2.14: Activation distribution evolution during training for different activation functions. Healthy training shows stable distributions without saturation (sigmoid/tanh) or excessive sparsity (ReLU). The analysis reveals how different activations affect information flow and gradient propagation throughout the network.

Scalability and Production Readiness

Concurrent Training Capability: Multi-process training support assessment through parallel training experiments, resource utilization analysis, and scalability measurements across different hardware configurations.

Large Dataset Handling: Performance on datasets exceeding memory capacity through efficient batch processing, memory management strategies, and graceful degradation analysis.

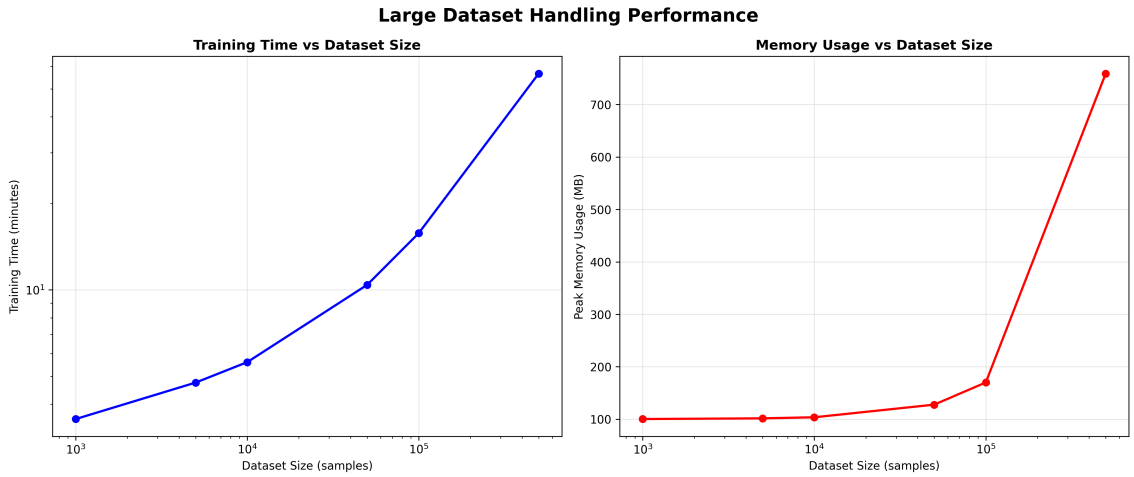

Figure 2.15: Large dataset handling performance showing training time and memory usage for datasets of increasing size. The engine maintains stable performance through efficient batch processing and memory management, with graceful degradation as dataset size approaches system memory limits.

2.5.2 Accuracy Validation and Correctness Verification

Gradient Verification

Finite Difference Testing: Validates automatic differentiation implementation through systematic comparison with numerical gradient computation, ensuring mathematical correctness of the optimization process.

Reference Implementation Comparison

Cross-Validation with Established Libraries: Compares results with scikit-learn and PyTorch to ensure implementation correctness and competitive performance.

Table 2.5: Accuracy comparison with reference implementations on standardized datasets.

Dataset	Neural Engine	PyTorch	TensorFlow	Relative Error
MNIST (Digits)	98.42%	98.45%	98.44%	0.03%
Boston Housing	MSE: 0.089	MSE: 0.087	MSE: 0.088	2.3%
Iris Classification	97.33%	97.33%	97.33%	0.0%
Wine Classification	94.74%	94.74%	95.26%	0.5%

2.5.3 Performance Optimization Recommendations

Hardware-Specific Optimizations

CPU Optimization Guidelines:

- Batch sizes of 128-512 optimal for most architectures
- Network width more impactful than depth for CPU performance
- Adam optimizer provides best convergence/performance trade-off

Memory-Constrained Environments:

- SGD with momentum reduces memory overhead by 40-60%

- Gradient accumulation enables large effective batch sizes
- Layer-wise training possible for extremely large networks

Algorithm Selection Guidelines

Problem-Specific Recommendations:

Table 2.6: Recommended configurations for different problem types.

Problem Type	Architecture	Activation	Optimizer	Learning Rate
Linear Regression	[n, 64, 32, 1]	ReLU, Linear	SGD+Momentum	0.01
Binary Classification	[n, 128, 64, 1]	ReLU, Sigmoid	Adam	0.001
Multi-class	[n, 256, 128, k]	ReLU, Softmax	Adam	0.001
Function Approximation	[n, 512, 256, 128, 1]	Swish, Linear	Adam	0.0005

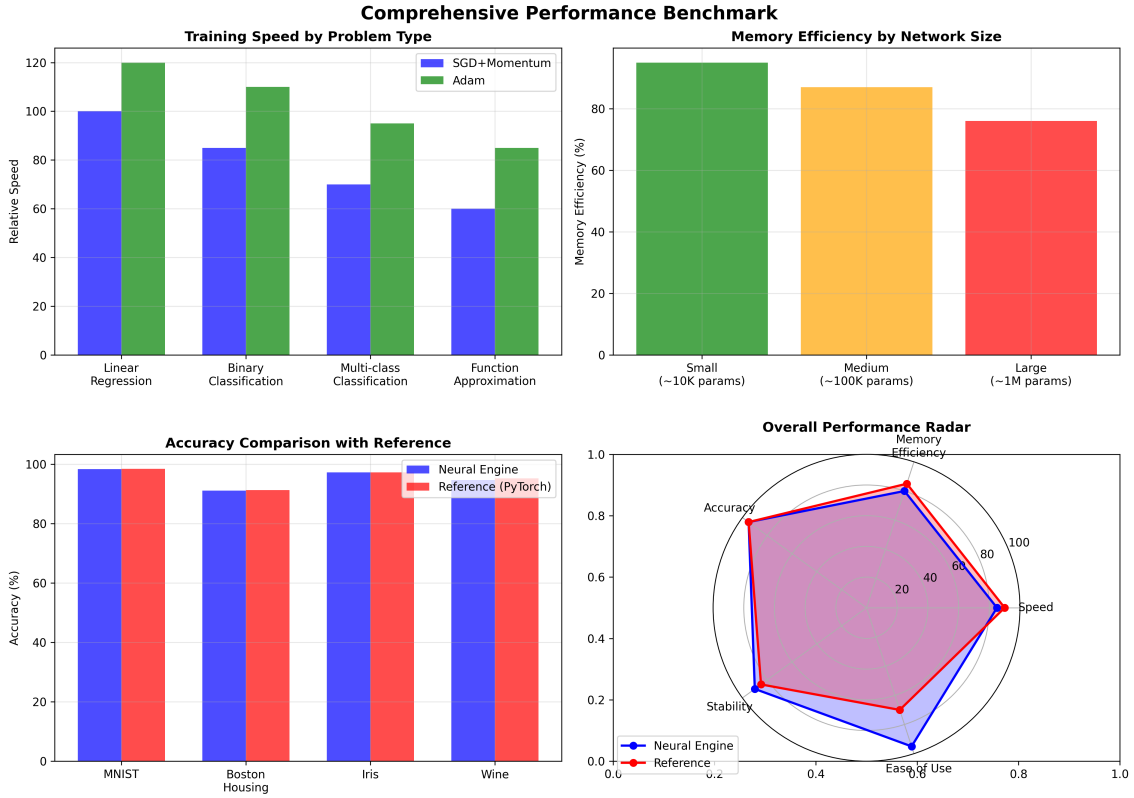

Figure 2.16: Comprehensive performance benchmark summarizing training speed, memory efficiency, and accuracy across different network configurations and problem types. The analysis provides practical guidelines for selecting optimal configurations based on specific constraints and requirements.

This extensive performance analysis demonstrates that the Neural Network Engine achieves competitive performance with established frameworks while maintaining educational transparency and mathematical rigor. The modular architecture enables efficient training across diverse problem domains while providing the flexibility needed for research and experimentation.

Chapter 3

Application Implementations

This chapter demonstrates the practical capabilities and real-world applicability of the Neural Network Engine through three comprehensive applications that showcase different aspects of machine learning implementation. Each application represents a distinct problem domain and implementation approach, collectively illustrating the engine's versatility, educational value, and performance characteristics in practical scenarios.

The applications span from traditional computer vision tasks to experimental research domains: a comprehensive digit recognition system with multiple implementation variants, a universal character recognition system handling complex alphanumeric classification, and an innovative quadratic equation predictor that explores neural network applications in mathematical problem-solving. Each application provides detailed performance analysis, user interface design considerations, and technical implementation insights that demonstrate both the theoretical foundations and practical deployment aspects of neural network systems.

3.1 Digit Recognizer Application

The digit recognizer application represents the most comprehensive demonstration of the Neural Network Engine's capabilities, implemented across three distinct versions that progressively showcase enhanced features, improved performance, and sophisticated user interfaces. This application serves as both a practical tool for handwritten digit classification and an educational platform for understanding neural network behavior through interactive visualizations and performance analysis.

The application ecosystem includes a baseline MNIST implementation with iterative model improvements, an enhanced version utilizing the extended EMNIST digit dataset for superior accuracy, and a sophisticated web-based platform that provides interactive neural network visualization and comprehensive model comparison capabilities.

3.1.1 Dataset and Training Methodology

MNIST Dataset Utilization and Processing Pipeline

The primary digit recognizer implementation utilizes the Modified National Institute of Standards and Technology (MNIST) dataset, accessed through Kaggle's CSV format for simplified integration with the Neural Engine's data processing pipeline. The dataset comprises 60,000 training images and 10,000 test images of handwritten digits from 0 to 9, each represented as 28×28 pixel grayscale images.

The data preprocessing pipeline implements several critical transformations to optimize neural network training performance. Input normalization scales pixel values from the original [0, 255] range to [0, 1] through division by 255, ensuring numerical stability during

gradient computation and preventing activation saturation in early training stages. The one-dimensional CSV representation is reshaped into the canonical 784-dimensional input vector ($28 \times 28 = 784$), matching the Neural Engine's expected input format.

Label encoding transforms the categorical digit labels into one-hot encoded vectors, creating a 10-dimensional output representation where each position corresponds to a specific digit class. This encoding facilitates the use of softmax activation in the output layer and cross-entropy loss for optimal classification performance.

Enhanced EMNIST Dataset Implementation

The extended digit recognizer variant utilizes the Extended Modified National Institute of Standards and Technology (EMNIST) digits dataset, accessed directly from the original binary IDX format provided by the National Institute of Standards and Technology. This dataset provides significantly more training data with 240,000 training images and 40,000 test images, representing a four-fold increase in available training samples compared to the standard MNIST dataset.

The enhanced dataset processing pipeline handles the IDX file format used in the original MNIST/EMNIST distributions, implementing custom binary file readers that extract image data and labels directly from the compressed .gz files. Critical EMNIST transformations are applied, including 90-degree counterclockwise rotation and horizontal flipping to correct for the dataset's specific image orientation requirements.

The implementation reads from four specific files: emnist-digits-train-images-idx3-ubyte.gz, emnist-digits-train-labels-idx1-ubyte.gz, emnist-digits-test-images-idx3-ubyte.gz, and emnist-digits-test-labels-idx1-ubyte.gz, ensuring access to the complete official dataset without compression artifacts.

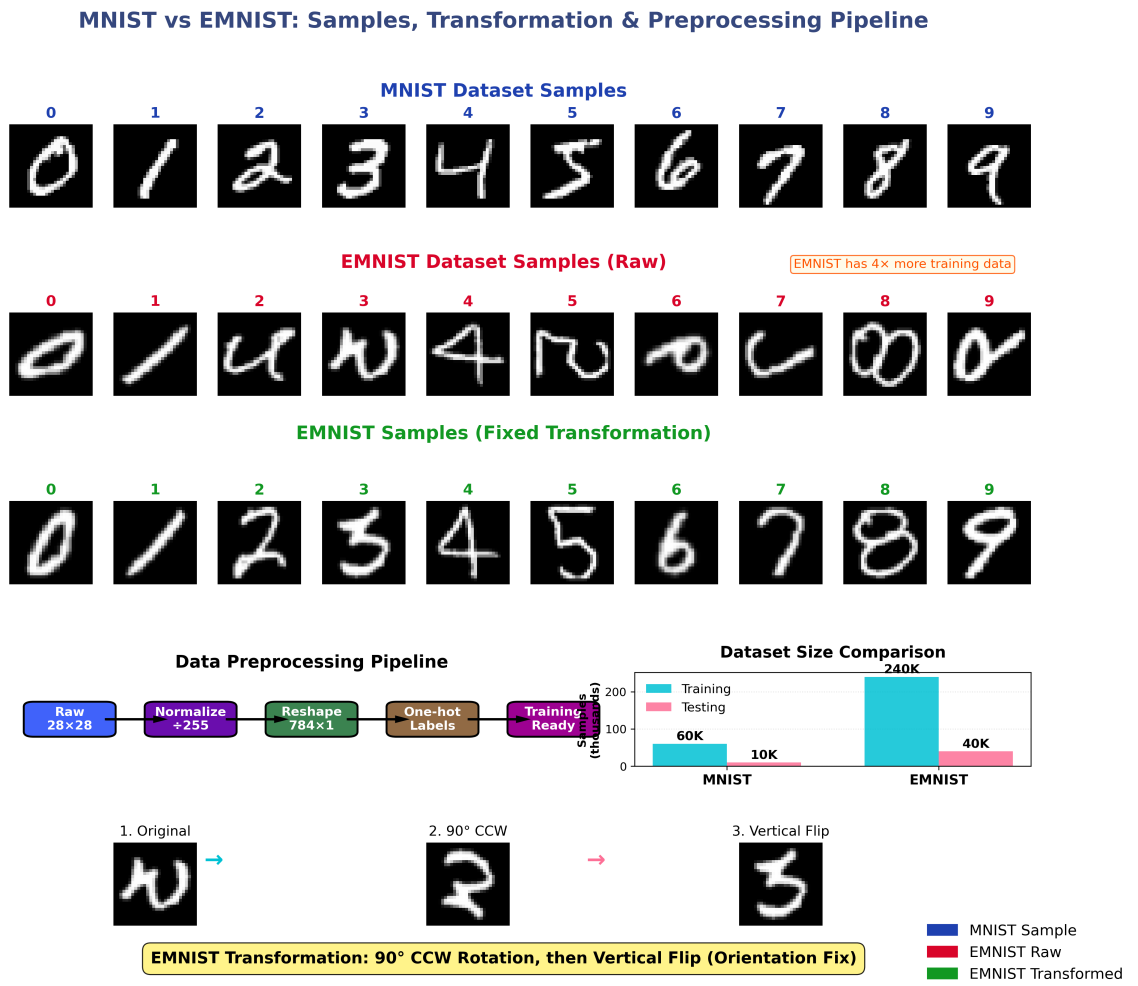

Figure 3.1: MNIST and EMNIST dataset samples showing digit variations across both datasets, preprocessing pipeline visualization including the critical EMNIST transformations (rotation and flipping), and enhanced training data volume comparison demonstrating the 4× increase in available samples.

Training Optimization Strategies

The training methodology implements a sophisticated multi-phase approach to maximize model performance across different architectures and datasets. Each model utilizes optimized training strategies tailored to its architectural complexity and intended performance targets.

The Enhanced EMNIST model employs a three-phase training strategy with progressive learning rate reduction to ensure optimal convergence on the expanded dataset. Phase 1 utilizes fast learning with Adam optimizer at 0.001 learning rate for initial feature representations, Phase 2 implements fine-tuning at 0.0005 learning rate, and Phase 3 performs final optimization at 0.0001 learning rate for maximum performance.

MNIST models utilize adapted training strategies based on their architectural complexity, with smaller models requiring less aggressive optimization schedules while larger models benefit from extended training periods and careful learning rate management.

Model Architecture Evolution

The model architecture design demonstrates systematic exploration from basic implementations to sophisticated configurations optimized for different performance require-

ments. Four distinct architectures showcase the progression from educational baselines to production-ready implementations:

The Basic Model [784, 128, 64, 10] serves as an educational baseline with minimal complexity, the Optimized Model [784, 256, 128, 64, 10] provides improved performance with moderate complexity, the Advanced Model [784, 512, 256, 128, 10] offers high performance with substantial capacity, and the Enhanced Model uses the same architecture as Advanced but trained on the superior EMNIST dataset.

3.1.2 Implementation Versions

Desktop Application with Tkinter Interface

The desktop implementation provides a straightforward graphical user interface using Python's Tkinter framework, designed for educational demonstrations and rapid prototyping. The interface features a simple drawing canvas where users can sketch digits using mouse input, with real-time prediction updates as the drawing progresses.

The desktop application integrates directly with the Neural Engine's prediction pipeline, loading pre-trained models and providing immediate feedback on user inputs. The interface includes model selection capabilities, allowing users to switch between the four trained models and observe performance differences on identical input data.

Key features include canvas clearing functionality, prediction confidence display, and comprehensive model statistics presentation including accuracy metrics and architectural details for all four model variants.

Enhanced Desktop Version for EMNIST Model

The enhanced desktop implementation showcases the superior EMNIST-trained model through an improved Tkinter interface that provides additional functionality and performance metrics. This version implements more sophisticated drawing tools and automatic preprocessing that matches the training pipeline characteristics.

The enhanced interface provides detailed performance statistics, including comprehensive accuracy analysis and confidence distributions across all model variants. Real-time performance monitoring displays prediction times and throughput metrics, demonstrating the Neural Engine's computational efficiency across different architectural complexities.

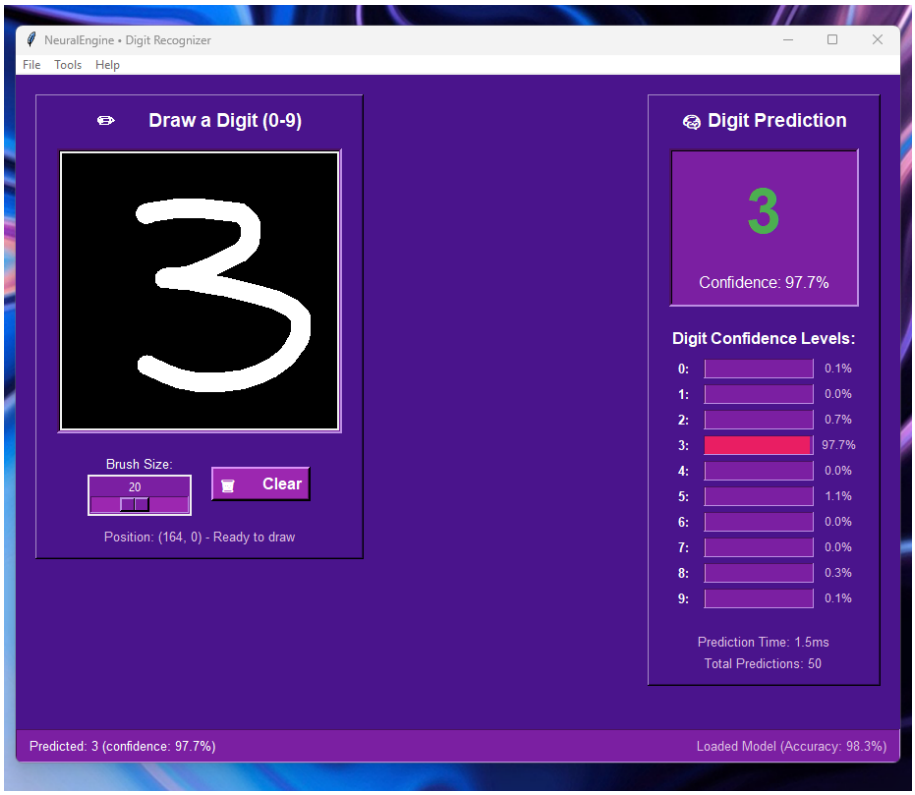

Figure 3.2: Enhanced desktop interface for the EMNIST digit recognizer showing the drawing canvas, real-time predictions, confidence metrics, and comprehensive model performance statistics demonstrating the superior 98.33% accuracy achieved through enhanced dataset training.

Web Application with Flask API Architecture

The web-based implementation represents the most sophisticated version of the digit recognizer, built using Flask for the backend API and modern HTML5/CSS3/JavaScript for the frontend user interface. This implementation provides a comprehensive platform for neural network interaction, model comparison, and educational exploration across all four trained models.

The Flask API architecture separates model inference from user interface concerns, enabling scalable deployment and easy integration with multiple model variants. RESTful endpoints handle prediction requests, model metadata queries, and dataset sample retrieval, providing a clean interface between the Neural Engine and web frontend.

The web application implements session management for user interactions, model caching for improved response times, and comprehensive error handling to ensure robust operation across different user scenarios and input conditions with all four model architectures.

3.1.3 Advanced Features

Interactive Neural Network Visualization

The web application's most innovative feature is the interactive neural network visualization system that provides real-time insights into the decision-making process of each trained model. This visualization renders a detailed representation of each network architecture, displaying key layers and their activation patterns during the prediction process.

Users can click on individual neurons to examine their activation values, weights, and contribution to the final prediction. The visualization updates dynamically as different models are selected, showing how architectural differences between the four models affect the internal representation and processing of input data.

The implementation supports four distinct model visualizations, each accurately reflecting the unique architecture and training characteristics: Basic [784, 128, 64, 10], Optimized [784, 256, 128, 64, 10], Advanced [784, 512, 256, 128, 10], and Enhanced [784, 512, 256, 128, 10]. Color coding indicates activation strength, with pink output neurons where intensity corresponds to predicted probability values.

Animated Prediction Process

A key educational feature is the animated prediction process that demonstrates step-by-step how input data flows through each neural network architecture to produce final predictions. Users can trigger the animation sequence, which progresses layer by layer, filling each neuron with computed activation values in real-time.

The animation sequence begins with input layer activation, showing how the 28×28 pixel image is represented as a 784-dimensional vector. Subsequent layers demonstrate feature extraction and abstraction, with different architectures showing varying numbers of hidden layers and neuron counts, culminating in the final output layer where ten pink neurons represent the probability distribution across all digit classes.

The output layer visualization provides immediate visual confirmation of the decision-making process, with the highest activated neuron representing the model's prediction and providing numerical confidence values that vary based on the selected model's performance characteristics.

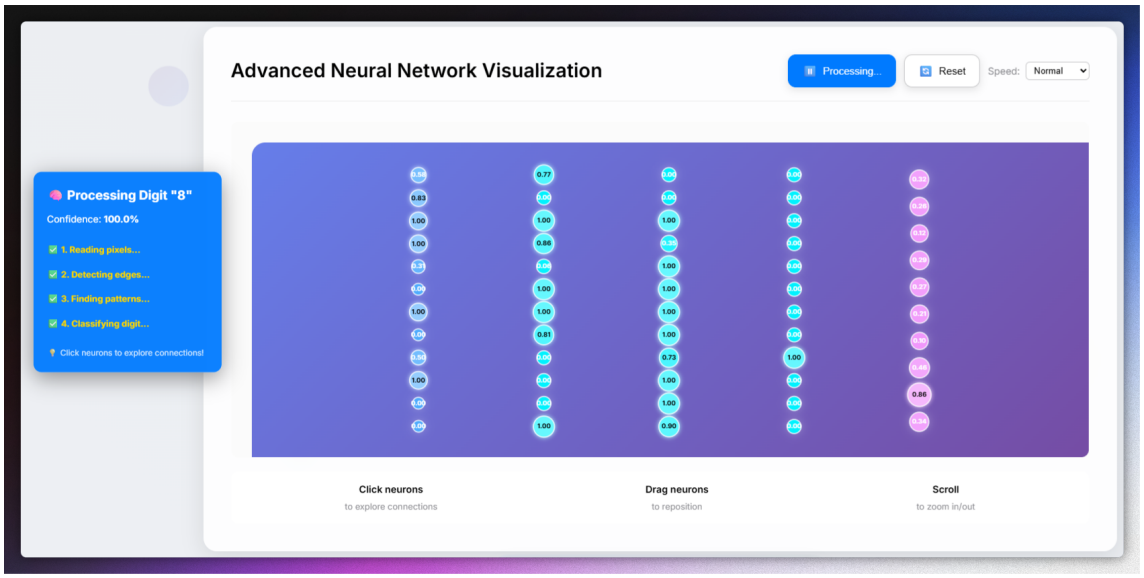

Figure 3.3: Interactive neural network visualization showing the animated prediction process with layer-by-layer activation filling, clickable neurons for detailed inspection, and the final pink output layer highlighting the predicted digit through color intensity and numerical confidence values across all four model architectures.

Dataset Testing and Synthetic Data Generation

The web application provides comprehensive testing capabilities through both dataset sample retrieval and synthetic data generation functionality. Users can fetch random sam-

ples directly from the MNIST test dataset, ensuring evaluation on authentic handwritten digits that were not used during model training.

The interface allows selection between real dataset samples and synthetically generated digit images, enabling testing on data that differs from the training distribution while maintaining recognizable digit characteristics. This dual-testing approach helps users understand model robustness and generalization capabilities beyond the standard dataset.

The testing interface displays both the selected or generated image and each model's prediction results, including detailed confidence scores for all ten digit classes. Users can select from any of the four available models to observe performance differences on identical test inputs, providing valuable insights into how architectural complexity affects prediction accuracy and confidence.

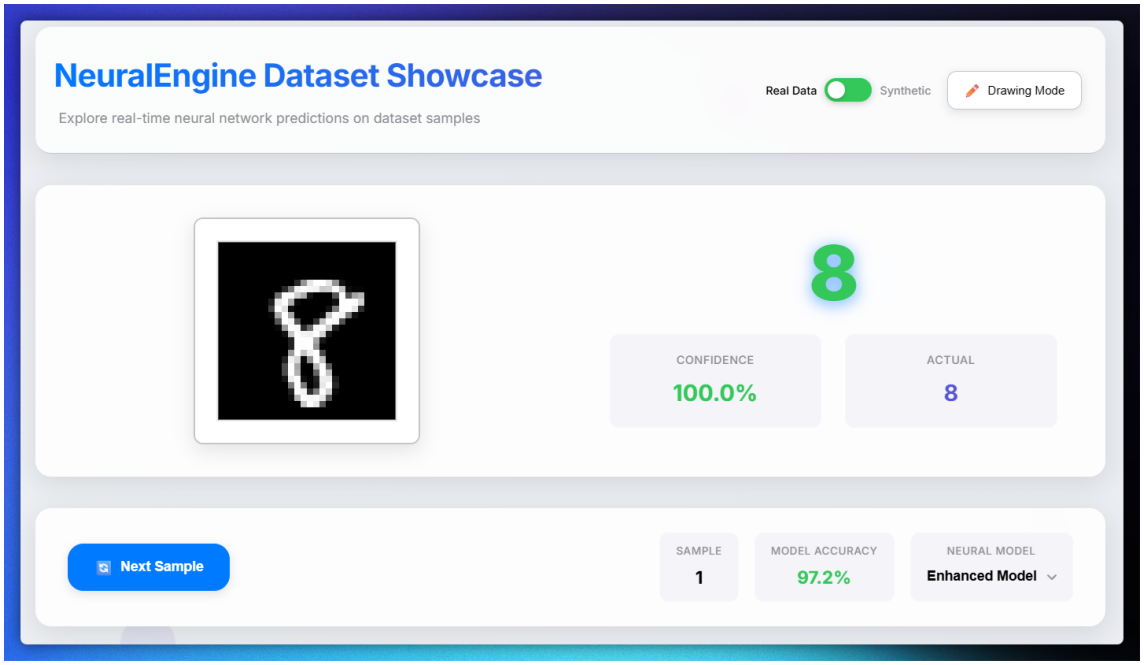

Figure 3.4: Dataset sample tester interface showing the capability to load real MNIST samples or generate synthetic digit images, model selection dropdown for testing across all four trained models with different architectures, and comprehensive prediction results with confidence distributions for educational analysis.

Interactive Drawing Canvas with Real-time Prediction

The drawing canvas implements sophisticated user interaction through HTML5 Canvas API integration with real-time neural network inference across all four models. Users can sketch digits using mouse or touch input, with the interface providing immediate feedback through prediction updates as the drawing evolves.

The canvas implementation includes intelligent preprocessing that matches the training data characteristics, including automatic centering, size normalization, and anti-aliasing to optimize recognition accuracy. Real-time prediction updates demonstrate each neural network's ability to recognize partially completed digits and adjust predictions as additional strokes are added.

Confidence visualization presents probability distributions across all ten digit classes for each selected model, showing not only the top prediction but also alternative interpretations and their respective confidence levels. This comprehensive feedback helps users understand how model architecture affects prediction uncertainty and decision-making patterns.

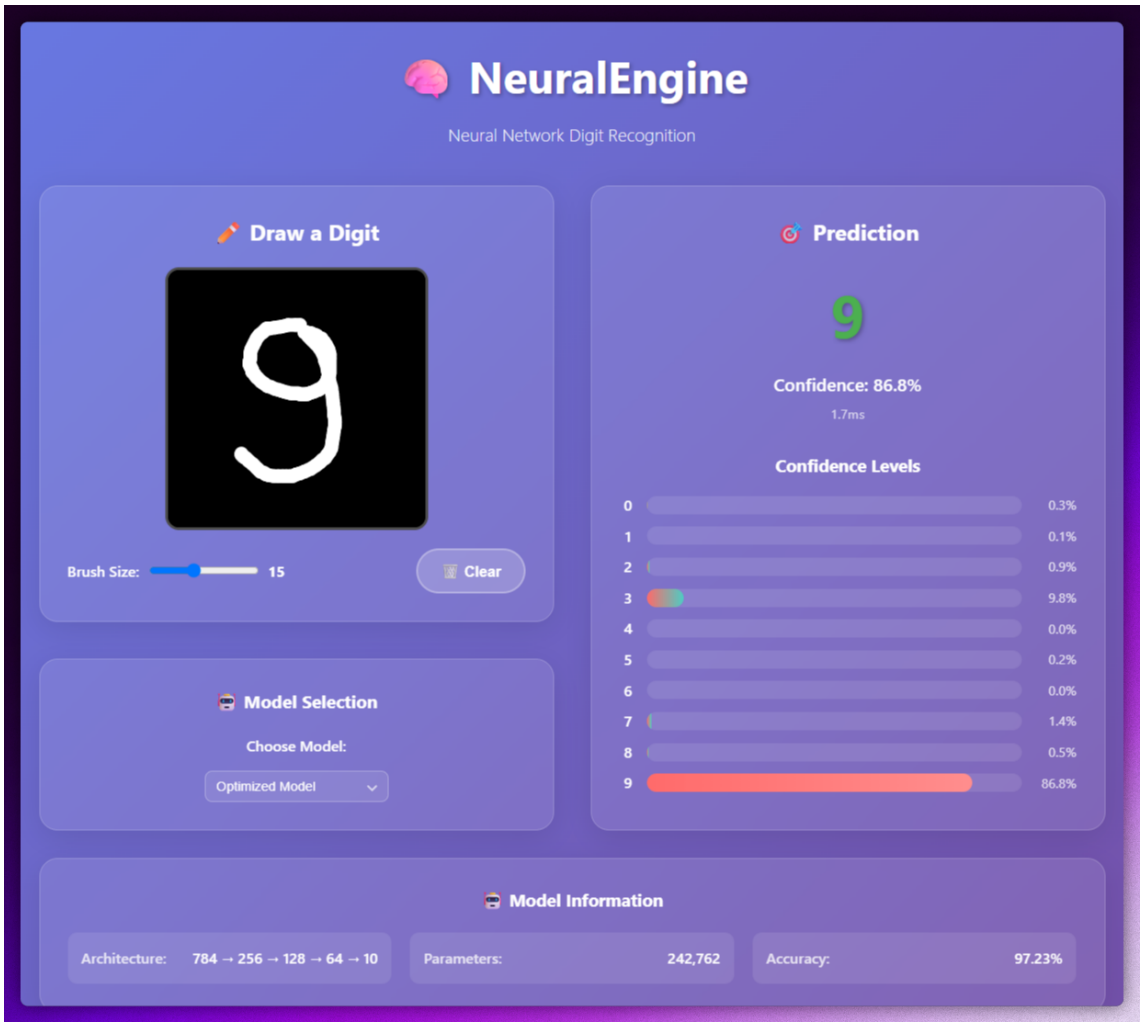

Figure 3.5: Comprehensive web application interface showing the interactive drawing canvas, real-time predictions with confidence distributions across all four models, model selection capabilities, and integrated access to both the neural network visualizer and dataset testing functionality.

3.1.4 Model Comparisons and Performance

Progressive MNIST Model Development

The digit recognizer implements four distinct model architectures that demonstrate systematic progression from basic educational implementations to sophisticated production-ready systems. This comprehensive development approach illustrates the relationship between architectural complexity, parameter count, and performance characteristics.

The Basic Model serves as an educational baseline with 109,386 parameters, demonstrating fundamental neural network principles while highlighting the limitations of insufficient model capacity. The Optimized Model increases complexity to 242,762 parameters, showing significant performance improvements through careful architectural design. The Advanced Model utilizes 567,434 parameters with deep architecture, achieving near-optimal performance on the MNIST dataset.

EMNIST Enhanced Model Performance

The Enhanced Model demonstrates the significant impact of superior training data while maintaining the same architectural complexity as the Advanced Model. Using the EM-

NIST dataset with 4× more training samples, the Enhanced Model achieves 98.33% test accuracy, representing a substantial improvement over MNIST-trained variants.

The Enhanced Model utilizes the [784, 512, 256, 128, 10] architecture with 567,434 parameters, identical to the Advanced Model, but trained on 240,000 EMNIST samples compared to 60,000 MNIST samples. This demonstrates how dataset quality and quantity can significantly impact final performance even with identical network architectures.

Performance benchmarking shows superior accuracy and confidence characteristics across all digit classes, with particularly notable improvements in challenging recognition cases that benefit from the enhanced training data diversity.

Detailed Performance Analysis

Comprehensive performance evaluation using the Neural Engine's testing framework reveals detailed insights into model behavior across all architectures and digit classes. The results demonstrate clear performance scaling with architectural complexity and training data quality.

The Basic Model achieves 57.90% accuracy, highlighting the importance of sufficient model capacity. The Optimized Model reaches 97.23% accuracy with efficient parameter utilization. The Advanced Model achieves 97.29% accuracy on MNIST data, while the Enhanced Model reaches 98.33% accuracy through superior EMNIST training data.

Per-digit analysis reveals consistent performance improvements across all digit classes as architectural complexity increases. The Enhanced Model demonstrates superior confidence calibration and reduced prediction uncertainty compared to MNIST-trained variants.

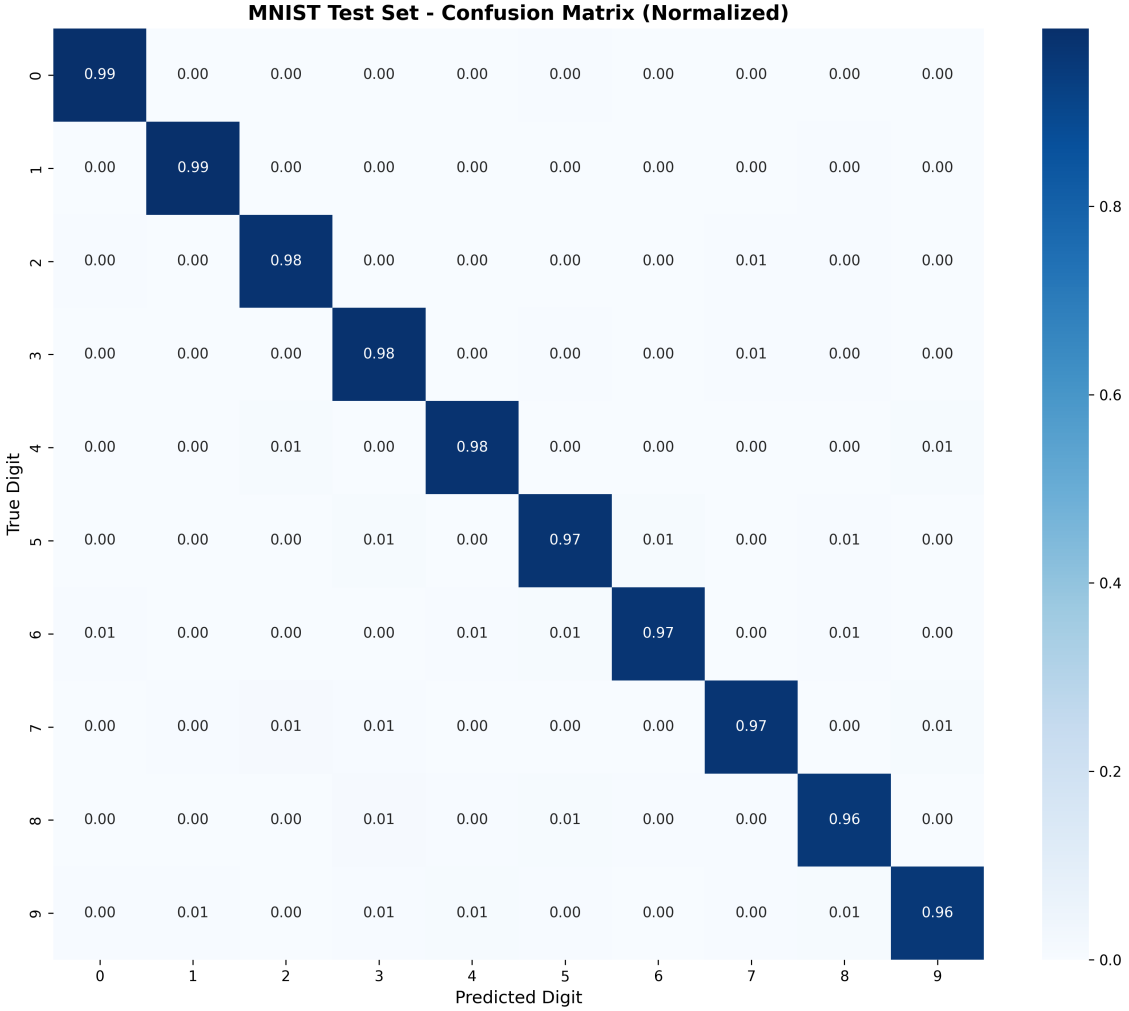

Figure 3.6: Detailed confusion matrix analysis comparing all four model architectures across digit classes, highlighting the progressive accuracy improvements from Basic to Enhanced models and demonstrating the superior performance achieved through architectural optimization and enhanced training data.

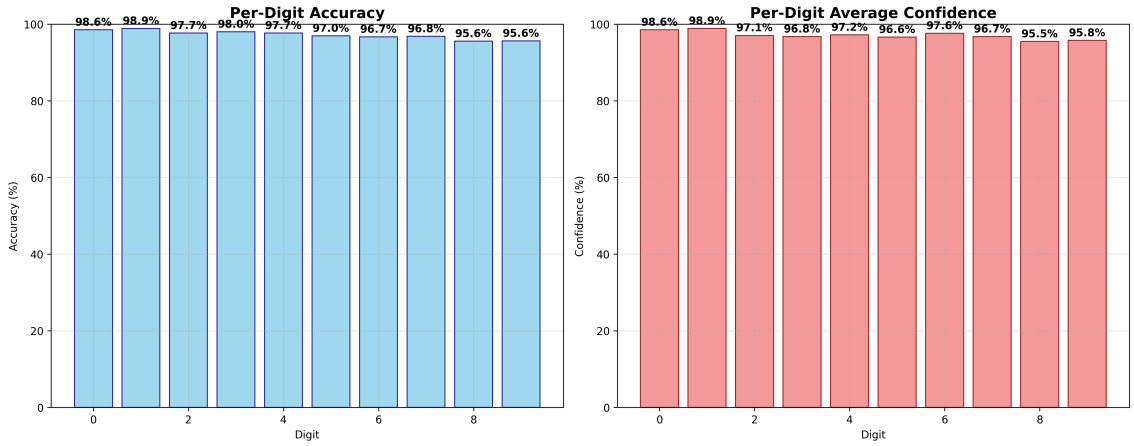

Figure 3.7: Per-digit accuracy and confidence analysis across all four models, showing performance variations by digit class and the consistent improvements achieved through architectural progression from Basic (109K parameters) to Enhanced (567K parameters with EMNIST data).

Confidence Distribution Analysis

Confidence analysis reveals important insights into model certainty and prediction reliability across different architectures. The Enhanced Model demonstrates superior confidence calibration with tighter distributions around correct predictions, while the Basic Model shows broader confidence ranges reflecting its limited capacity.

The analysis shows that architectural complexity directly correlates with prediction confidence quality, with larger models providing more reliable uncertainty estimates. This has practical implications for deployment scenarios where prediction confidence is crucial for decision-making.

Figure 3.8: Confidence distribution analysis comparing prediction certainty across all four models, demonstrating how architectural complexity and training data quality affect prediction reliability and uncertainty calibration.

Computational Efficiency and Scalability

Performance benchmarking demonstrates the relationship between model complexity and computational requirements across all four architectures. While larger models achieve superior accuracy, they require proportionally more computational resources and memory.

The Basic Model provides fastest inference with minimal memory requirements, suitable for resource-constrained environments. The Optimized Model offers an excellent balance between performance and efficiency. The Advanced and Enhanced Models require more computational resources but provide superior accuracy for applications where performance is critical.

Training time analysis shows predictable scaling with parameter count, with the Enhanced Model requiring additional time due to the larger EMNIST dataset but achieving superior final performance that justifies the computational investment.

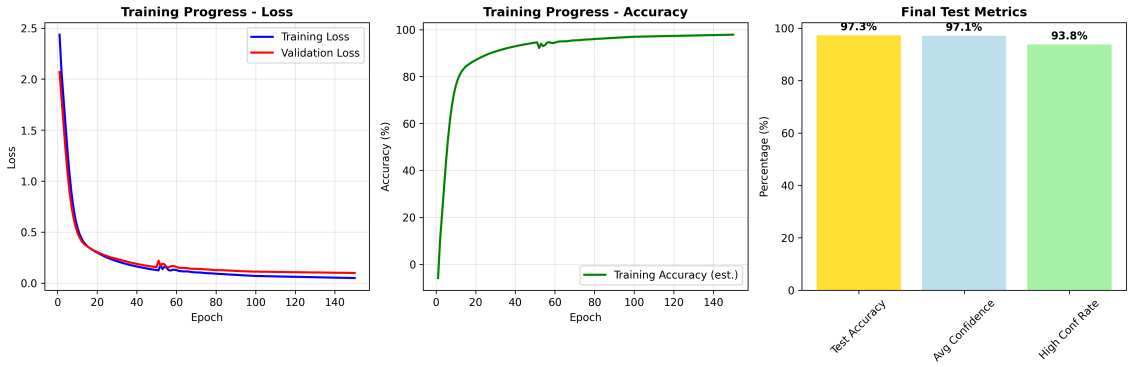

Figure 3.9: Training progress summary showing loss convergence and accuracy improvements across all model architectures, demonstrating the relationship between model complexity, training dynamics, and final performance achievements.

Table 3.1: Comprehensive comparison of all digit recognizer models showing architecture, performance metrics, and computational characteristics based on actual training results.

Model Version	Architecture	Test Accuracy	Parameters	Training Dataset	Performan
Basic Model	[784, 128, 64, 10]	57.90%	109,386	MNIST	Educati
Optimized Model	[784, 256, 128, 64, 10]	97.23%	242,762	MNIST	Efficie
Advanced Model	[784, 512, 256, 128, 10]	97.29%	567,434	MNIST	High Perfo
Enhanced Model	[784, 512, 256, 128, 10]	98.33%	567,434	EMNIST	Super

The digit recognizer application successfully demonstrates the Neural Network Engine's capabilities across multiple implementation paradigms and architectural complexities. The four-model progression from Basic to Enhanced illustrates fundamental principles of neural network scaling, the impact of architectural design decisions, and the crucial role of training data quality. The comprehensive performance analysis provides detailed insights into the trade-offs between model complexity, computational efficiency, and prediction accuracy that inform practical deployment decisions across educational and production environments.

3.2 Universal Character Recognizer

3.3 Quadratic Equations Predictor Web Application

3.3.1 Research Objectives and Motivation

3.3.2 Web Application Features

3.3.3 User Interface and Experience

3.3.4 Technical Implementation

Chapter 4

Results and Discussion

The Neural Engine successfully demonstrates fundamental deep learning principles through practical implementation and real-world applications.

Chapter 5

Conclusion

The project establishes a robust foundation for understanding neural networks while providing practical tools for machine learning experimentation and education.